

Computational Methods for Fluid Mechanics – lecture 4 Fluid-structure interaction

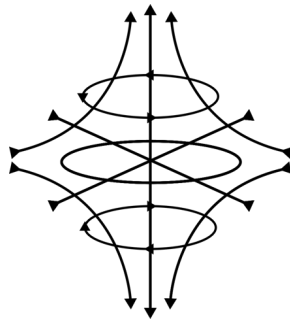
Johan Hoffman

Today

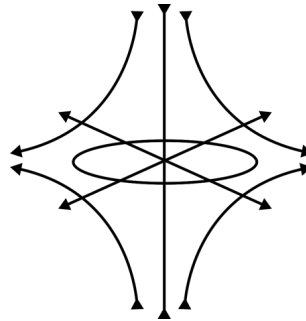
- Structure of turbulent flow
- Boundary layers, flow separation, and wall modelling.
- The structure of turbulent flow separation, analytical models, and the d'Alembert's paradox.
- Deforming domains and fluid-structure interaction

Some structures of incompressible flow

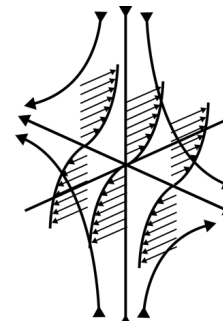
Vortex tube



Pancake



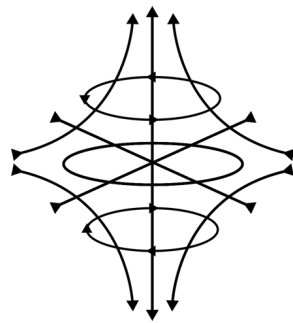
Shear layer



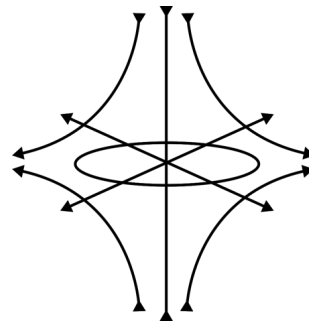
$$\nabla u \quad \begin{bmatrix} \lambda_R & 0 & 0 \\ 0 & \alpha & -\beta \\ 0 & \beta & \alpha \end{bmatrix} \quad \begin{bmatrix} 2\lambda_R & 0 & 0 \\ 0 & -\lambda_R & 0 \\ 0 & 0 & -\lambda_R \end{bmatrix} \quad \begin{bmatrix} 0 & 0 & \zeta \\ 0 & \lambda_R & 0 \\ 0 & 0 & -\lambda_R \end{bmatrix}$$

Some structures of incompressible flow

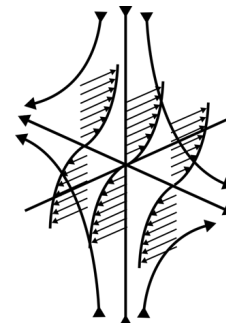
Vortex tube



Pancake



Shear layer



$$\nabla u \quad V \begin{bmatrix} \lambda_R & 0 & 0 \\ 0 & \lambda_C & 0 \\ 0 & 0 & \overline{\lambda_C} \end{bmatrix} V^* \begin{bmatrix} 2\lambda_R & 0 & 0 \\ 0 & -\lambda_R & 0 \\ 0 & 0 & -\lambda_R \end{bmatrix} \begin{bmatrix} 0 & 0 & \zeta \\ 0 & \lambda_R & 0 \\ 0 & 0 & -\lambda_R \end{bmatrix}$$

$$\lambda_C, \overline{\lambda_C} = \alpha \pm i\beta$$

Analysis of flow structures

- Vorticity $\omega = \nabla \times u$
- Double decomposition of velocity gradient tensor (VGT) into a strain rate tensor $S(u)$ and a spin tensor $\Omega(u)$ (used for Q-criterion, etc.)

$$\nabla u = \frac{1}{2} (\nabla u + \nabla u^T) + \frac{1}{2} (\nabla u - \nabla u^T) = S(u) + \Omega(u)$$

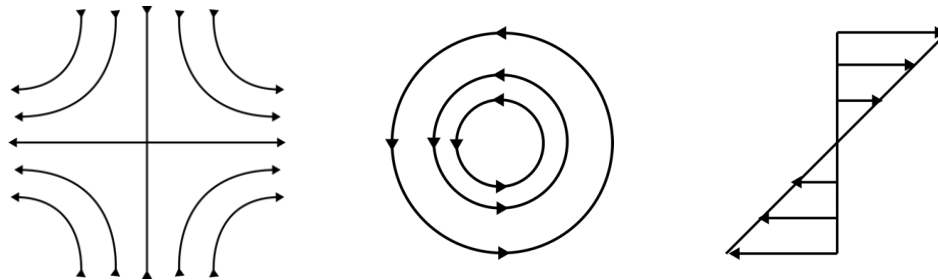
- These methods have a weakness: they do not distinguish shear flow from rotational flow and straining flow.
- Pointed out by V. Kolár [2007] in the context of vortex identification. Suggested a triple decomposition of VGT.
- Followed up by others [e.g. Liu et al. 2018, Keylock 2019, Nagata et al. 2020].

Triple decomposition of VGT

- Triple decomposition of the velocity gradient tensor

$$\nabla u = \nabla u_{strain} + \nabla u_{rotation} + \nabla u_{shear}$$

- Structure of fluid flow: strain + rotation + shear



Algebraic derivation

- Any square matrix A has a (non-unique) Schur factorization

$$A = UTU^*$$

U is unitary, T upper triangular with eigenvalues of A on the diagonal.

- Any normal square matrix is unitary diagonalizable (spectral theorem)

$$A = UDU^*$$

U is unitary with eigenvectors as columns, D diagonal with eigenvalues.

- Any square matrix A is decomposed into sum of a normal and a non-normal part.

$$A = UTU^* = UDU^* + U(T - D)U^*, \quad \|T - D\|_F^2 = \sum_i \sigma_i^2 - \sum_i |\lambda_i|^2$$

Algebraic derivation

- If A is a real matrix it has a real Schur form

$$A = QBQ^T$$

Q real and orthogonal, B real upper quasi-triangular with possible pairs of conjugate complex eigenvalues $(\lambda, \bar{\lambda})$ represented by real 2x2 block matrices on the diagonal with the same eigenvalues.
[Golub/Van Loan 1996]

$$\begin{bmatrix} \lambda & * \\ 0 & \bar{\lambda} \end{bmatrix} \rightarrow \begin{bmatrix} a & b \\ c & d \end{bmatrix}$$

- If $a = d$ and $cb < 0$, then the real Schur form is said to be in standardized form, which can be computed by standard methods. [Bai/Demmel 1993]

$$\begin{bmatrix} \alpha & \beta \\ \gamma & \alpha \end{bmatrix}, \quad \beta\gamma < 0, \quad \lambda, \bar{\lambda} = \alpha \pm \sqrt{\beta\gamma} = \alpha \pm i\sqrt{|\beta\gamma|}$$

Triple decomposition of VGT

- For the real 3x3 VGT we have a standardized real Schur form

$$\nabla u = Q \overline{\nabla u} Q^T = Q (\overline{\nabla u}_{diag} + \overline{\nabla u}_{skew} + \overline{\nabla u}_{nn}) Q^T = \nabla u_{sym} + \nabla u_{skew} + \nabla u_{nn}$$

- Assume $|\beta| > |\gamma|$, then with $\lambda_R + 2\alpha = 0$,

$$\overline{\nabla u} = \begin{bmatrix} \lambda_R & \varepsilon & \zeta \\ 0 & \alpha & \beta \\ 0 & \gamma & \alpha \end{bmatrix} = \begin{bmatrix} \lambda_R & 0 & 0 \\ 0 & \alpha & 0 \\ 0 & 0 & \alpha \end{bmatrix} + \begin{bmatrix} 0 & 0 & 0 \\ 0 & 0 & -\gamma \\ 0 & \gamma & 0 \end{bmatrix} + \begin{bmatrix} 0 & \varepsilon & \zeta \\ 0 & 0 & \beta + \gamma \\ 0 & 0 & 0 \end{bmatrix}$$

$$\|\nabla u_{sym}\|_F^2 = \lambda_R^2 + 2\alpha^2, \quad \|\nabla u_{skew}\|_F^2 = 2\gamma^2, \quad \|\nabla u_{nn}\|_F^2 = \sum_i \sigma_i^2 - \sum_i |\lambda_i|^2$$

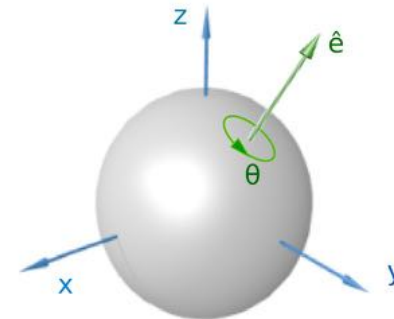
- This algebraic decomposition can be identified with a triple decomposition of VGT into strain, rotation and shear flow.
- Q represents a change of basis – how to interpret Q?

Euler's rotation theorem

- “When a sphere is moved around its center it is always possible to find a diameter whose direction in the displaced position is the same as in the initial position” (Euler, 1776)

- Rigid body rotational transformation represents the eigenvalue problem:

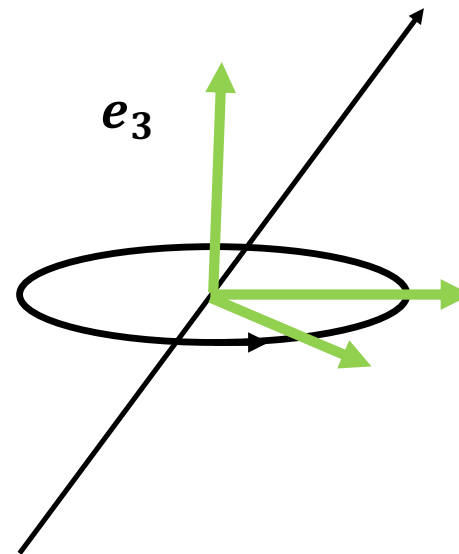
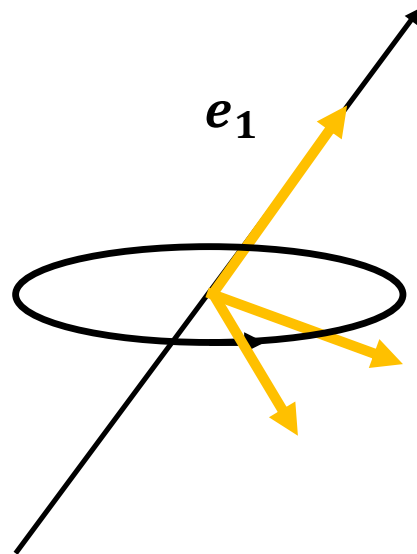
$$Rv = \lambda v \quad (\text{with } \lambda = 1)$$



[Wikipedia]

- Here it is natural to align Q with v.
- What about a general linear transformation?

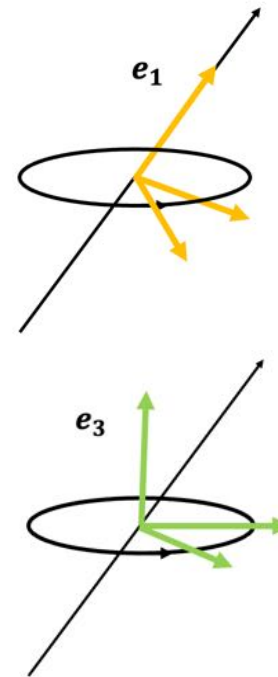
How to choose Q with shear?



How to choose Q with shear?

$$\nabla u = Q \overline{\nabla u} Q^T, \quad \overline{\nabla u} = \begin{bmatrix} \lambda_R & \varepsilon & \zeta \\ 0 & \alpha & \beta \\ 0 & \gamma & \alpha \end{bmatrix}$$

$$\nabla u = \hat{Q} \hat{\nabla u} \hat{Q}^T, \quad \hat{\nabla u} = \begin{bmatrix} \alpha & \hat{\beta} & \hat{\zeta} \\ \hat{\gamma} & \alpha & \hat{\varepsilon} \\ 0 & 0 & \lambda_R \end{bmatrix}$$



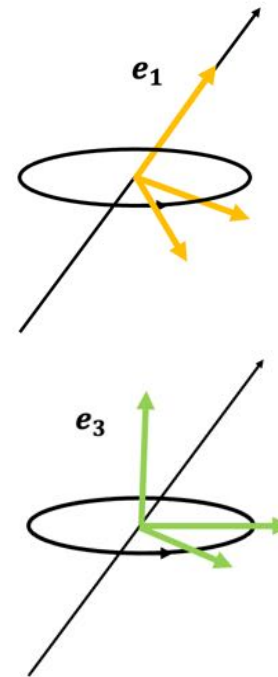
How to choose Q with shear?

$$v_R = Q e_1, \quad Q^T v_R = e_1$$

$$\nabla u v_R = Q \overline{\nabla u} Q^T v_R = Q \overline{\nabla u} e_1 = Q \lambda_R e_1 = \lambda_R v_R$$

$$\hat{v}_R = \hat{Q} e_3, \quad \hat{Q}^T \hat{v}_R = e_3$$

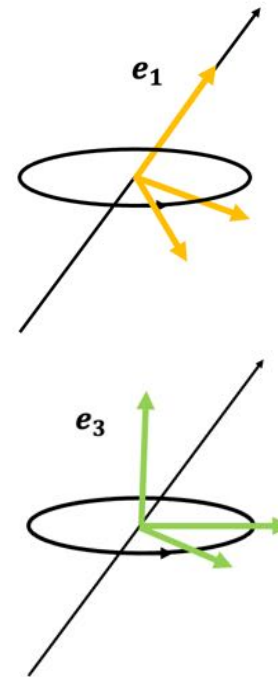
$$\nabla u \hat{v}_R = \hat{Q} \widehat{\nabla u} \hat{Q}^T \hat{v}_R = \hat{Q} \widehat{\nabla u} e_3 = \hat{Q} \begin{bmatrix} \hat{\zeta} \\ \hat{\varepsilon} \\ \lambda_R \end{bmatrix} = \hat{Q} \begin{bmatrix} \hat{\zeta}/\lambda_R \\ \hat{\varepsilon}/\lambda_R \\ 1 \end{bmatrix}$$



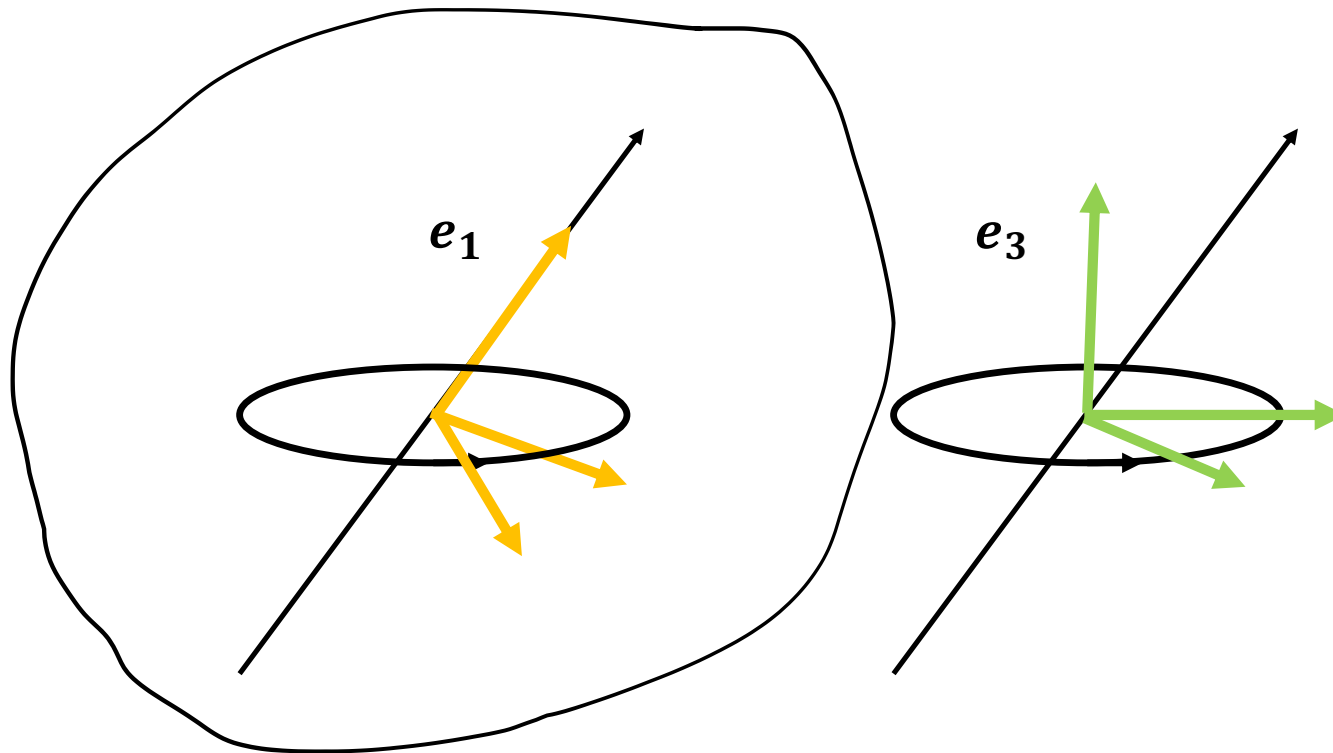
How to choose Q with shear?

$$\widehat{\nabla u} \begin{bmatrix} \hat{\xi} \\ \hat{v} \\ 0 \end{bmatrix} = \begin{bmatrix} \alpha & \hat{\beta} & \hat{\zeta} \\ \hat{\gamma} & \alpha & \hat{\varepsilon} \\ 0 & 0 & \lambda_R \end{bmatrix} \begin{bmatrix} \hat{\xi} \\ \hat{v} \\ 0 \end{bmatrix} = \begin{bmatrix} \alpha \hat{\xi} + \hat{\beta} \hat{v} \\ \hat{\gamma} \hat{\xi} + \alpha \hat{v} \\ 0 \end{bmatrix}$$

$$\overline{\nabla u} \begin{bmatrix} 0 \\ \xi \\ \nu \end{bmatrix} = \begin{bmatrix} \lambda_R & \varepsilon & \zeta \\ 0 & \alpha & \beta \\ 0 & \gamma & \alpha \end{bmatrix} \begin{bmatrix} 0 \\ \xi \\ \nu \end{bmatrix} = \begin{bmatrix} \varepsilon \xi + \zeta \nu \\ \alpha \xi + \beta \nu \\ \gamma \xi + \alpha \nu \end{bmatrix}$$



For consistency – go with Euler!



Stability analysis of NSE

- Navier-Stokes equations

$$\begin{aligned}\frac{\partial u}{\partial t} + (u \cdot \nabla)u + \nabla p - \nu \Delta u &= f \\ \nabla \cdot u &= 0\end{aligned}$$

- Perturbation equation, adjoint equation, vorticity equation

$$\begin{aligned}\frac{\partial u'}{\partial t} + (u \cdot \nabla)u' + (u' \cdot \nabla)U + \nabla p' - \nu \Delta u' &= P(\cdot), & \nabla \cdot u' &= 0 \\ -\frac{\partial \varphi}{\partial t} - (u \cdot \nabla)\varphi + \nabla U^T \varphi + \nabla \theta - \nu \Delta \varphi &= M(\cdot), & \nabla \cdot \varphi &= 0 \\ \frac{\partial \omega}{\partial t} + (u \cdot \nabla)\omega - (\omega \cdot \nabla)u - \nu \Delta \omega &= \Omega(\cdot), & \nabla \cdot \omega &= 0\end{aligned}$$

Stability analysis of NSE

- All have the same type of stability property ($\phi = \varphi, u', \omega$)

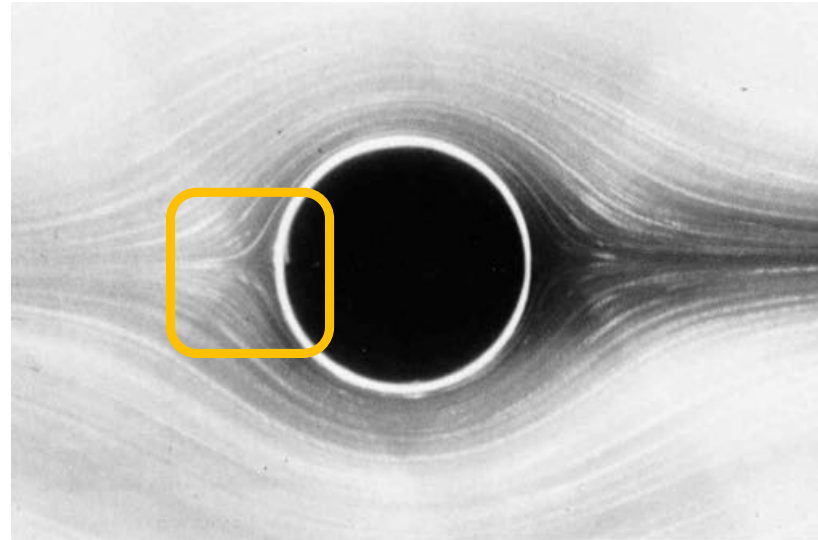
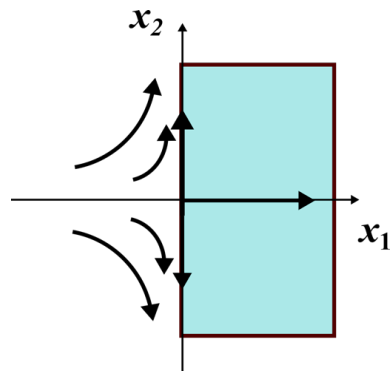
$$\frac{1}{2} \frac{d}{dt} \|\phi\|^2 \pm \int_{\Omega} \phi^T \nabla u \phi \, dx = -\nu \|\nabla \phi\|^2 + S(\phi)$$

- The key term which determines the stability is the integral

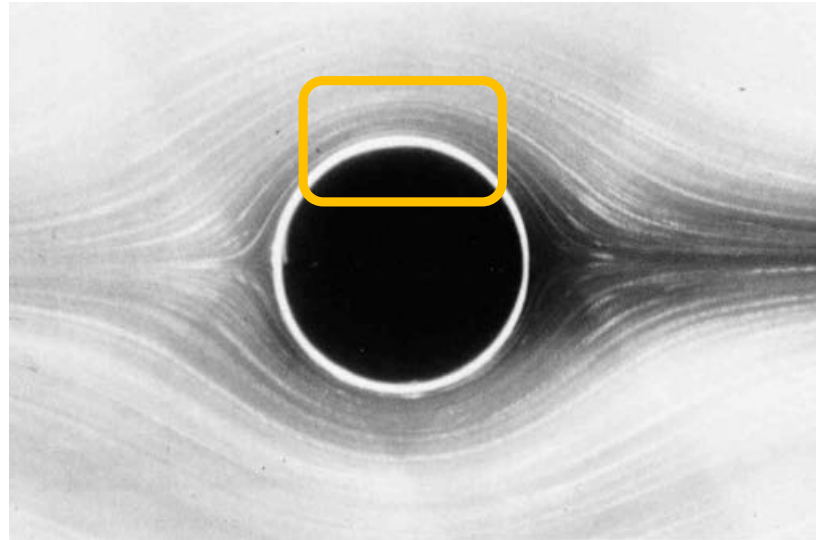
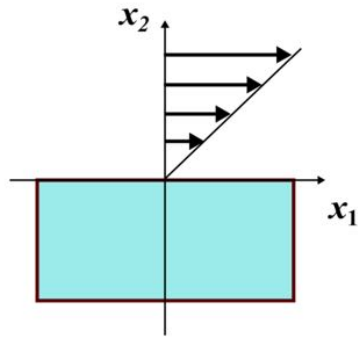
$$\int_{\Omega} \phi^T \nabla u \phi \, dx = \int_{\Omega} \phi^T (\nabla u_{sym} + \nabla u_{skew} + \nabla u_{nn}) \phi \, dx = \int_{\Omega} \phi^T (\nabla u_{sym} + \nabla u_{nn}) \phi \, dx$$

- Rigid body rotational flow is stable (stable vortices)
- Shear flow is linearly unstable (e.g. shear layer roll-up)
- Straining flow exponentially unstable (e.g. vortex stretching)

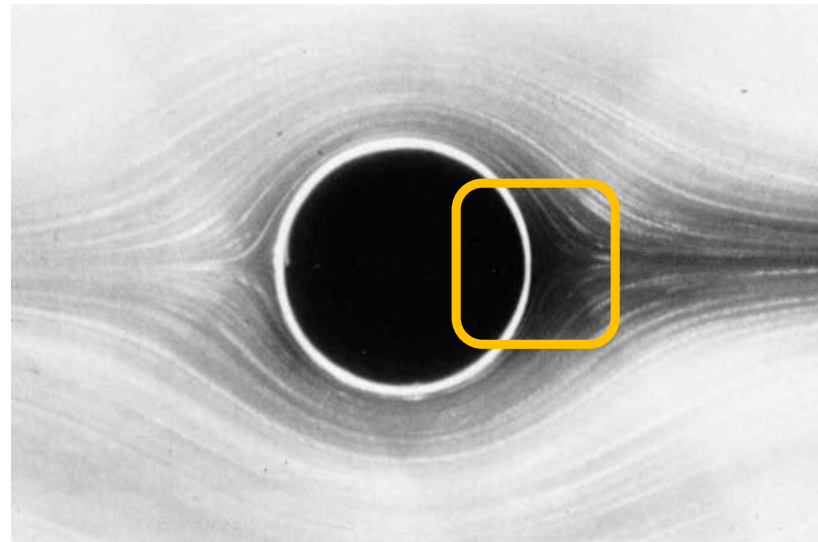
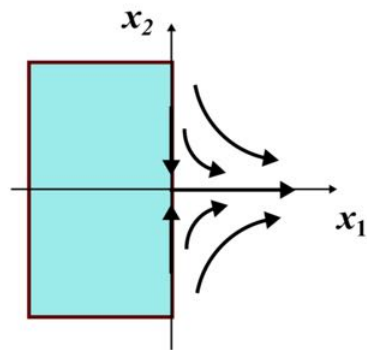
Cylinder ($Re = 0.16$) – attachment point



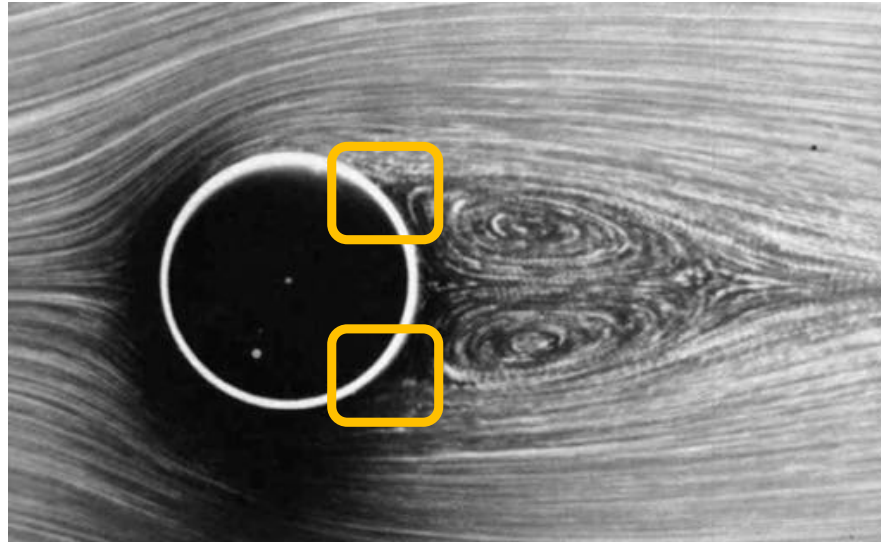
Cylinder ($Re = 0.16$) – boundary layer



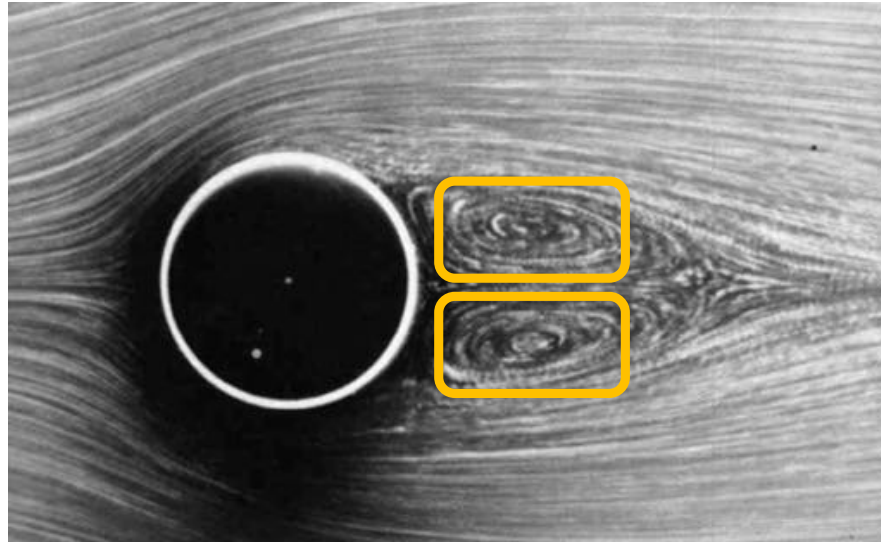
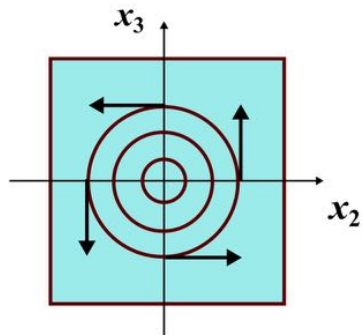
Cylinder ($Re = 0.16$) – separation point



Cylinder ($Re = 26$) – 2 separation points



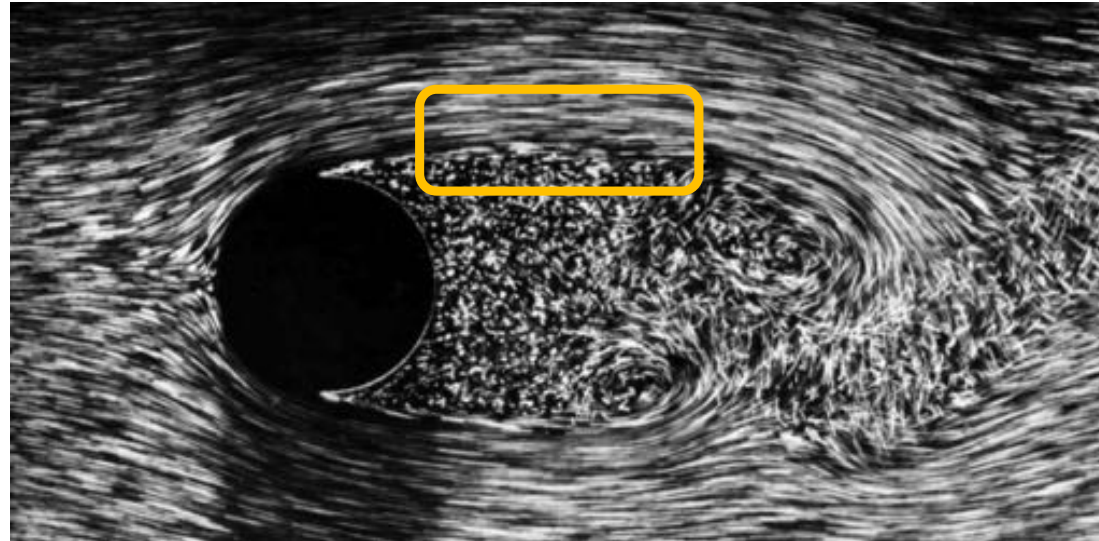
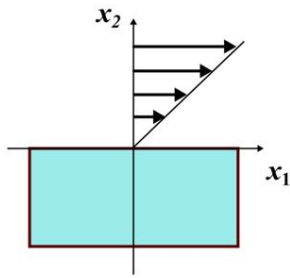
Cylinder ($Re = 26$) – 2 vortices



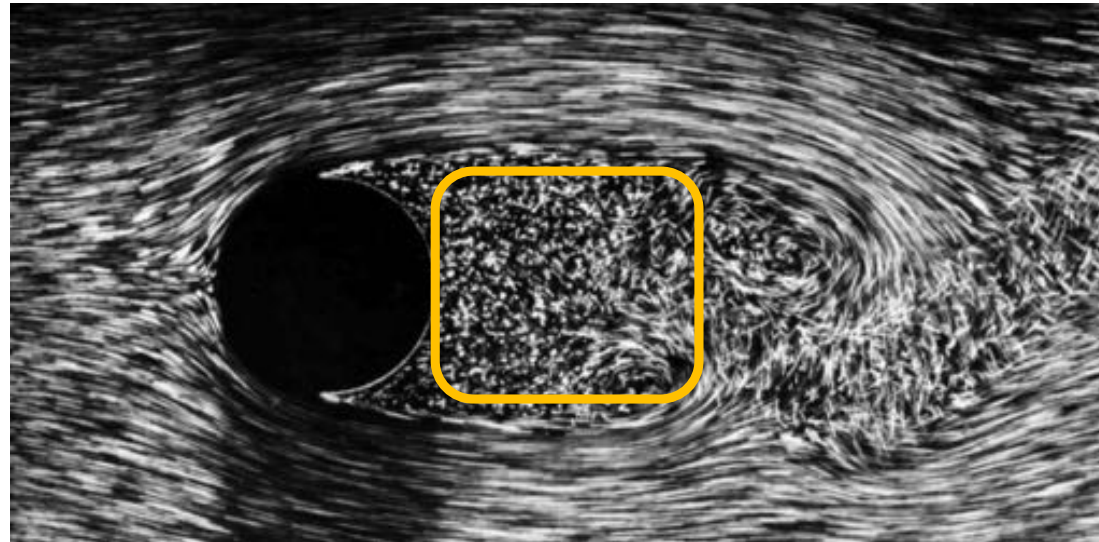
Cylinder ($Re = 300$) – Karman vortex street



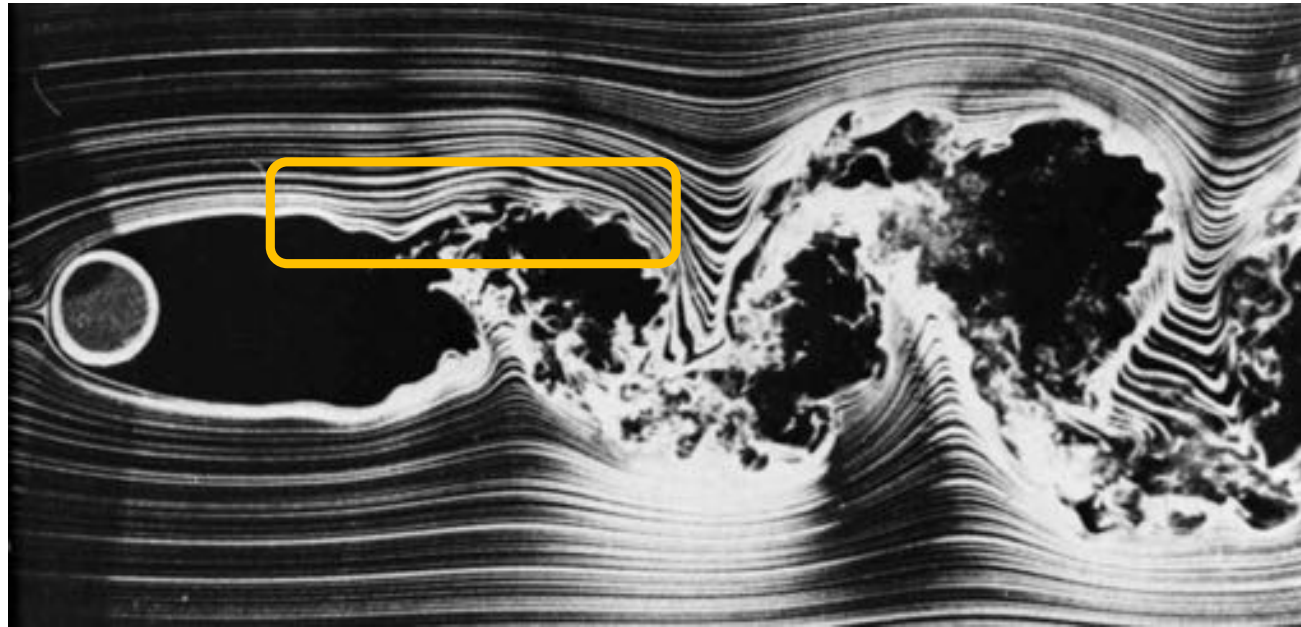
Cylinder ($Re = 2000$) – shear layer



Cylinder ($Re = 2000$) – 3D turbulent wake



$Re = 10\,000$ – turbulent shear layers

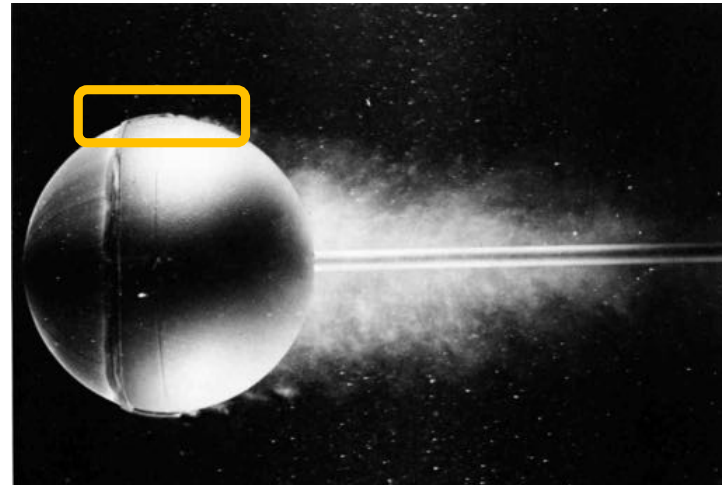
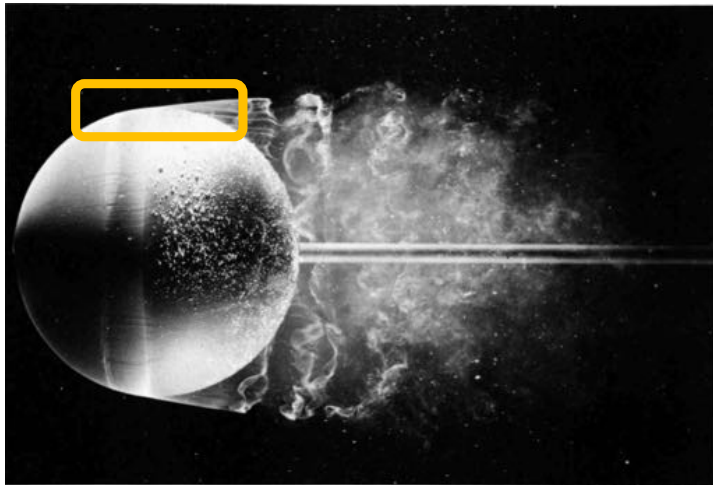


Kelvin-Helmholtz shear layer instability

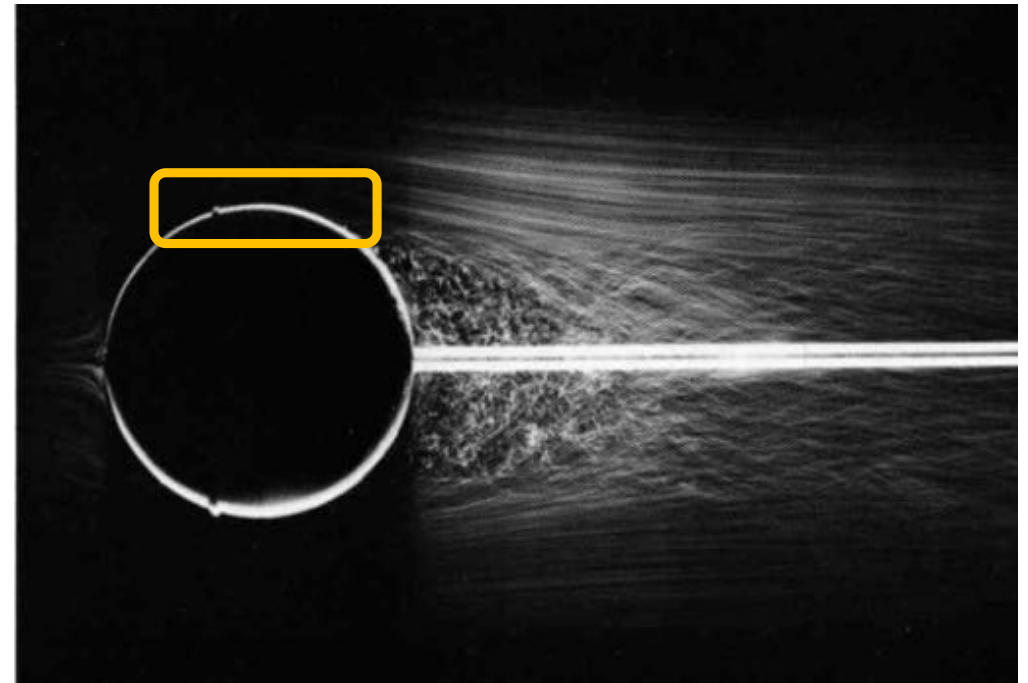
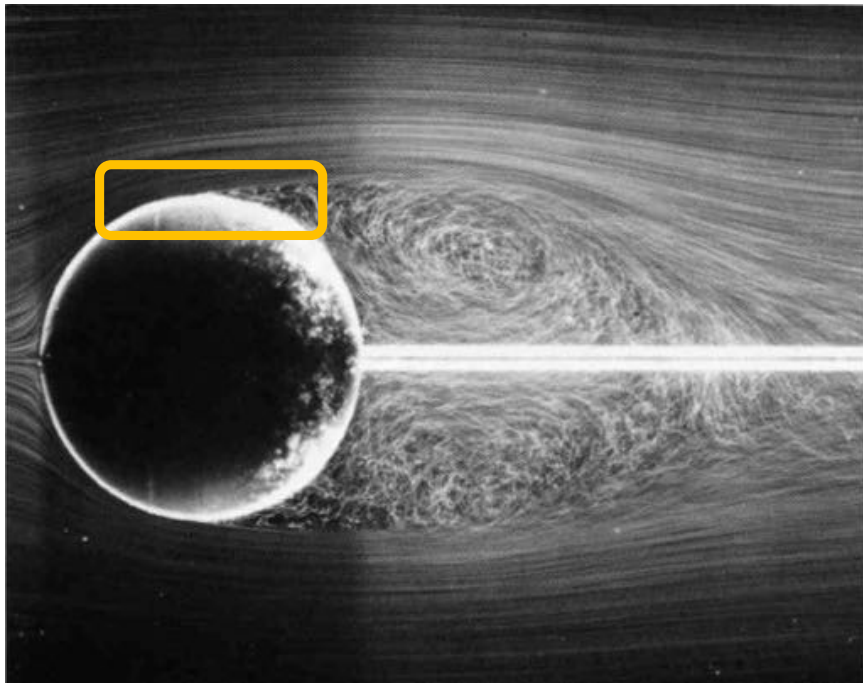


[Wikipedia]

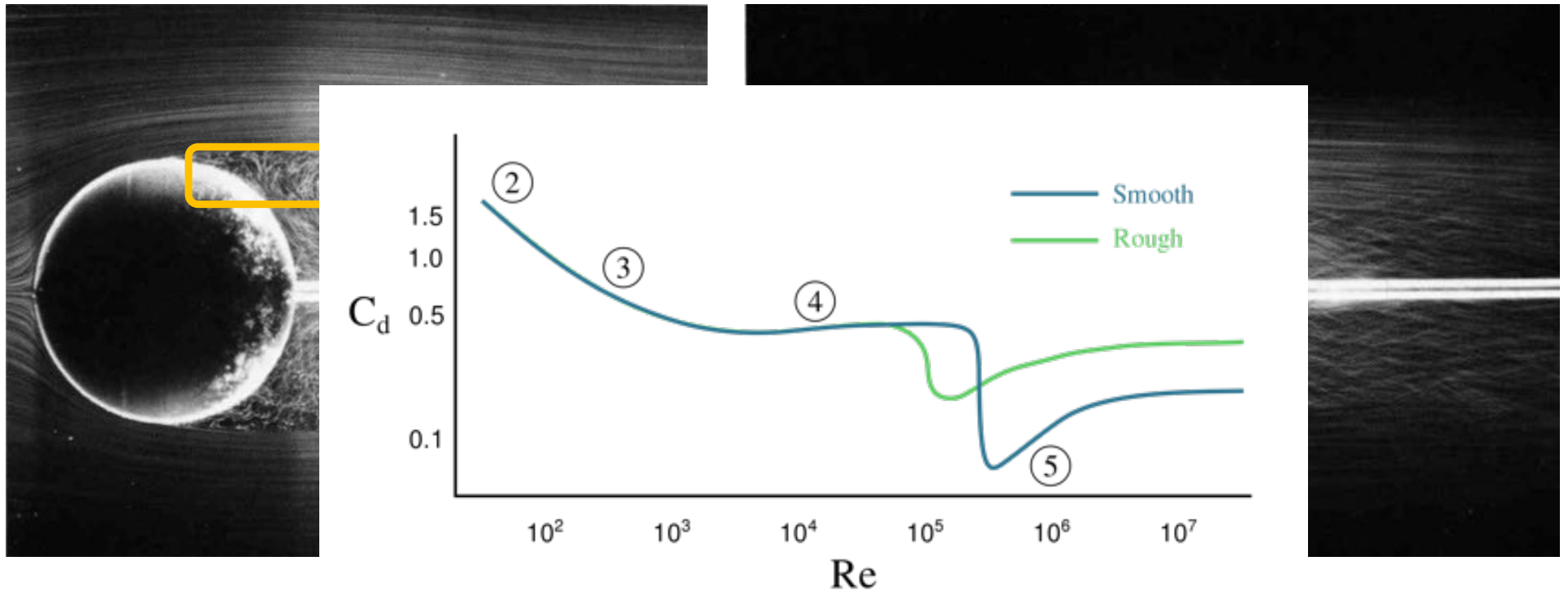
$Re = 30\,000$ - turbulent boundary layer



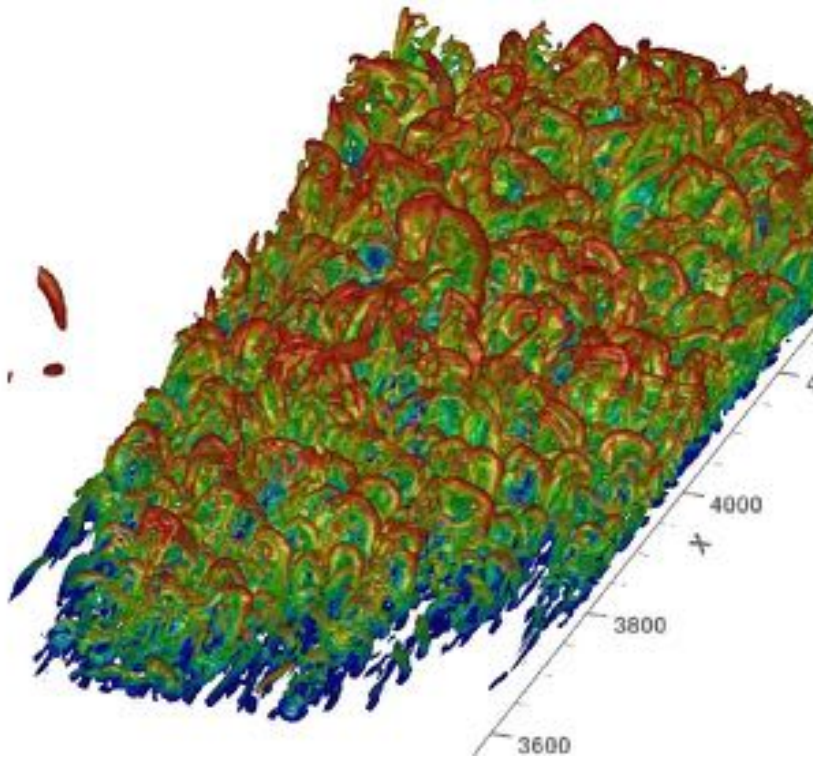
Sphere: $Re = 15\,000$ vs $30\,000$
turbulent boundary layers (drag crisis)



Sphere: $Re = 15\ 000$ vs $30\ 000$
turbulent boundary layers (drag crisis)



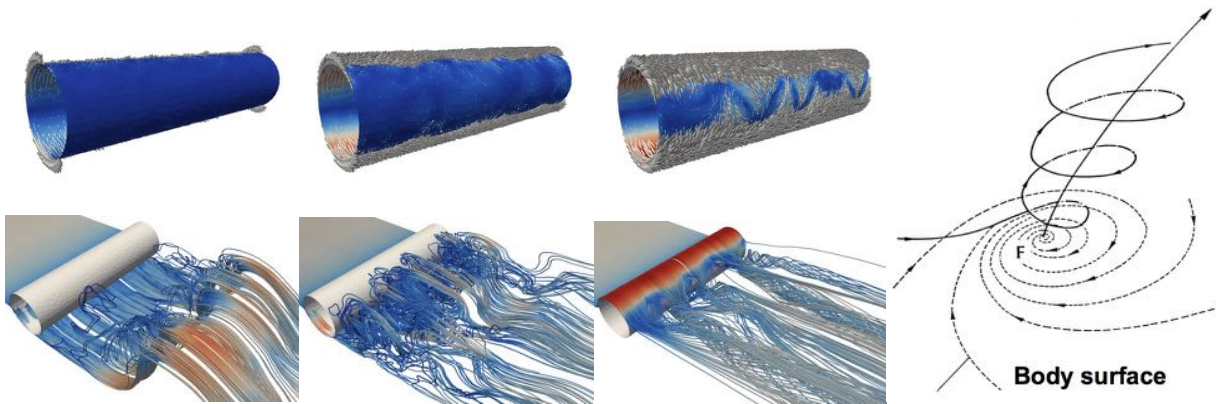
Turbulent boundary layer



- [Simulation tbl](#) [Schlatter et al.]

Turbulent separation by a slip bc

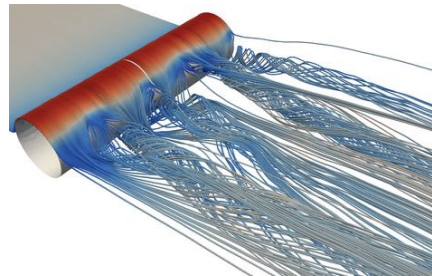
- For high Re: model effect of turbulent boundary layers as a slip boundary condition (zero skin friction)
- Effectively computing dissipative Euler solutions by GLS
- Example: high Re flow past circular cylinder (drag crisis)
- Resolution of d'Alembert's paradox: potential flow unstable in 3D



Turbulent separation by a slip bc

Consistent with experiments:

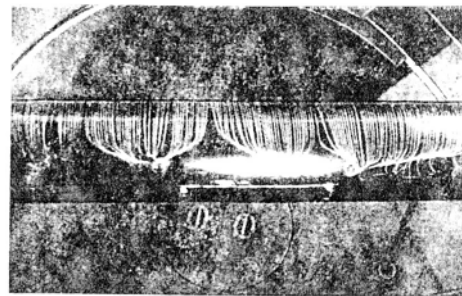
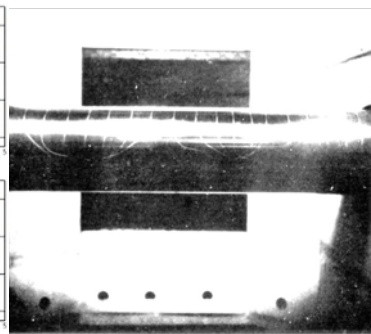
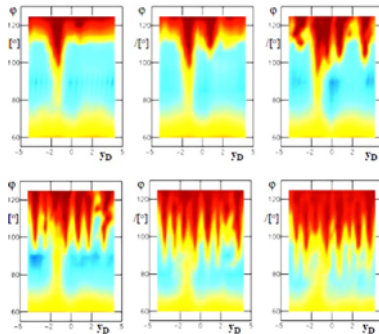
- Drag crisis: drag drops by a factor 4
- Streamwise vortices form stable cells in zig zag pattern
- Cell diameter \sim cylinder diameter



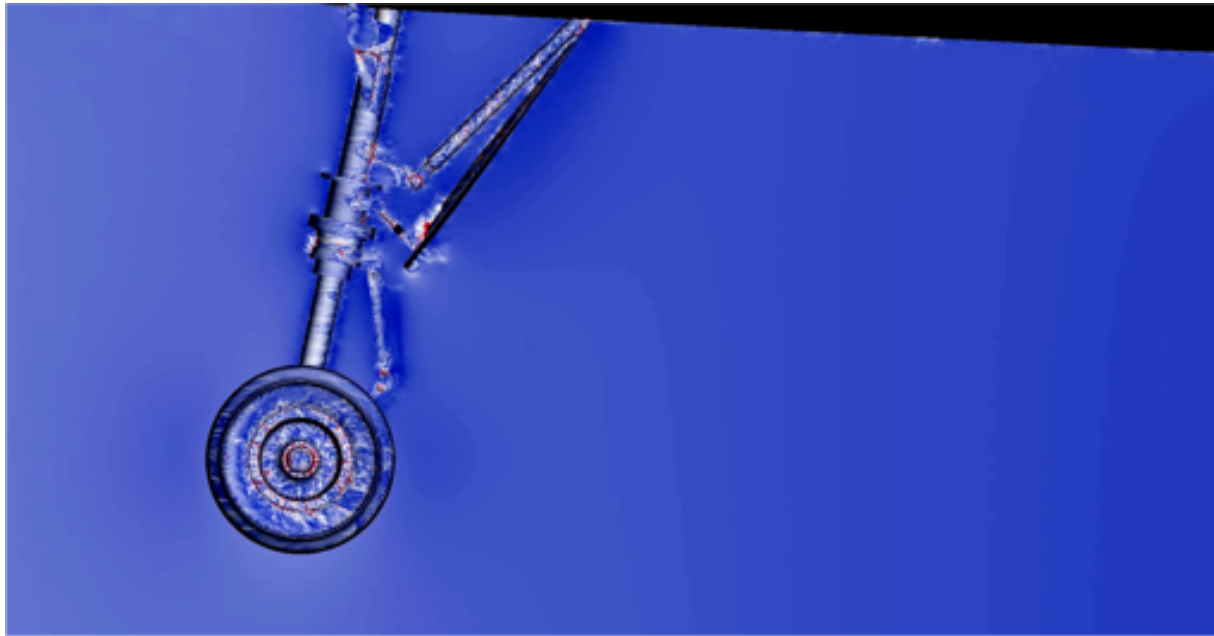
[Gölling DLR 2001]

[Humphreys JFM 1960]

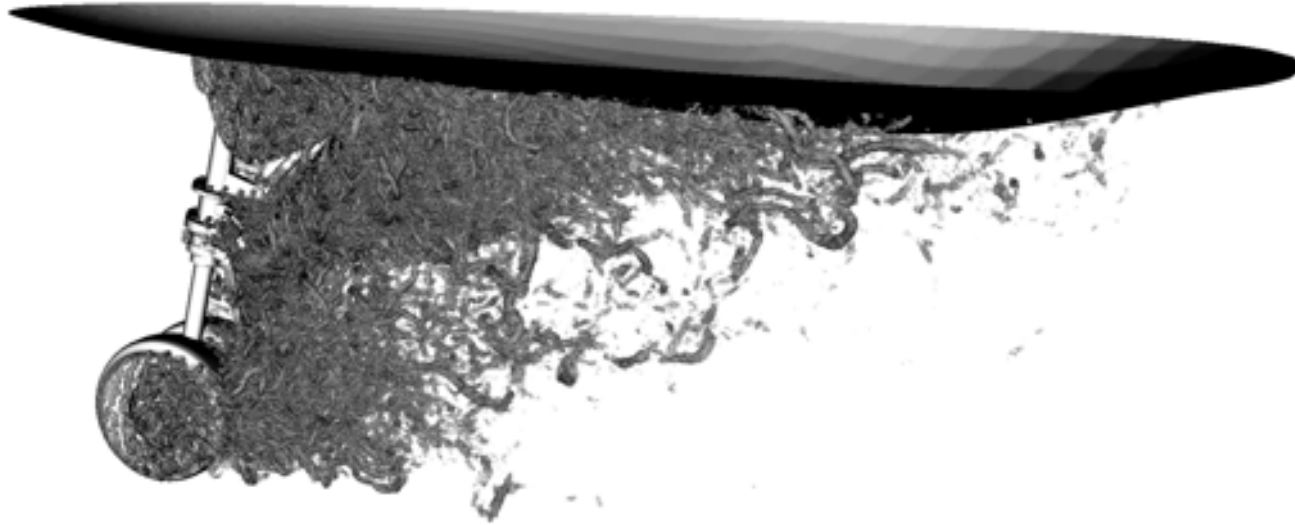
[Korotkin 1976]



Simulation of airflow past landing gear



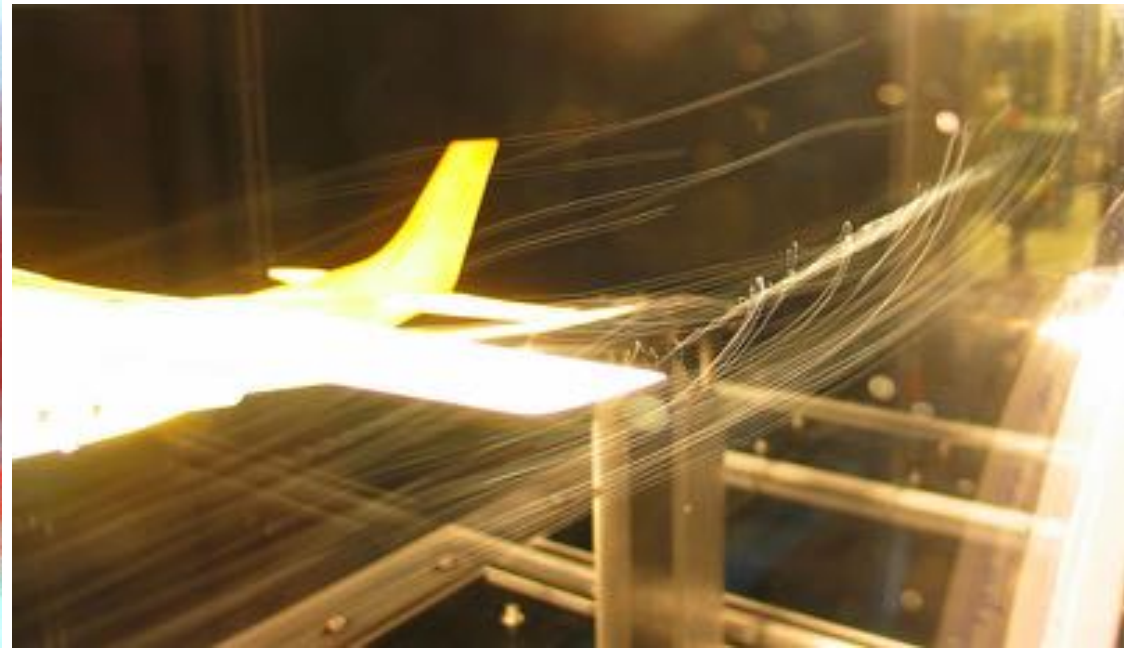
Turbulent vortices (lambda2 criterion)



Delayed separation and vortex structures



[https://en.wikipedia.org/wiki/File:Airplane_vortex_edit.jpg]



[https://sv.m.wikipedia.org/wiki/Fil:Cessna_182_model-wingtip-vortex.jpg]

Delayed separation - downwash



[<https://i.redd.it/7yj9h0x2h9f61.jpg>]



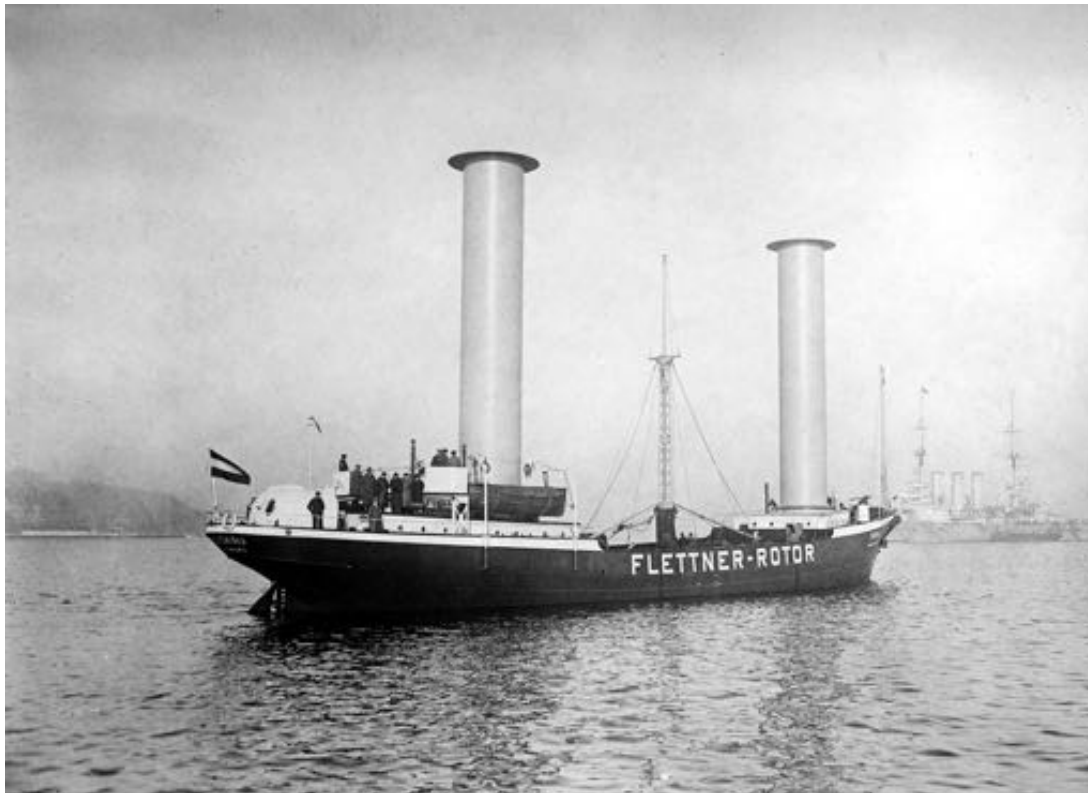
[<https://www.grc.nasa.gov/www/k-12/airplane/downwash.html>]

Magnus effect – downwash through rotation



[https://en.wikipedia.org/wiki/Magnus_effect#/media/File:Magnus-anim-canette.gif]

Buckau- Flettner rotor ship 1924



[https://en.wikipedia.org/wiki/Flettner_rotor#/media/File:Buckau_Flettner_Rotor_Ship_LOC_37764u.jpg]

Grace- Flettner rotor ship 2019



Grace - Flettner rotor ship 2019

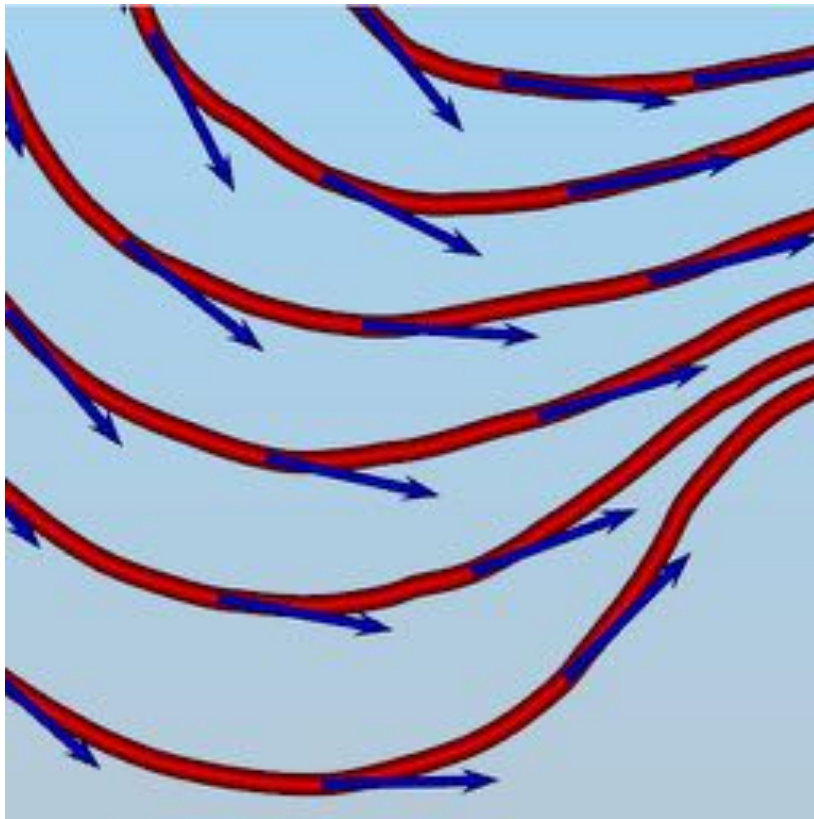


Flow visualization: pathlines



[https://en.wikipedia.org/wiki/Streamlines,_streaklines,_and_pathlines#/media/File:Kaberneeme_campfire_site.jpg]

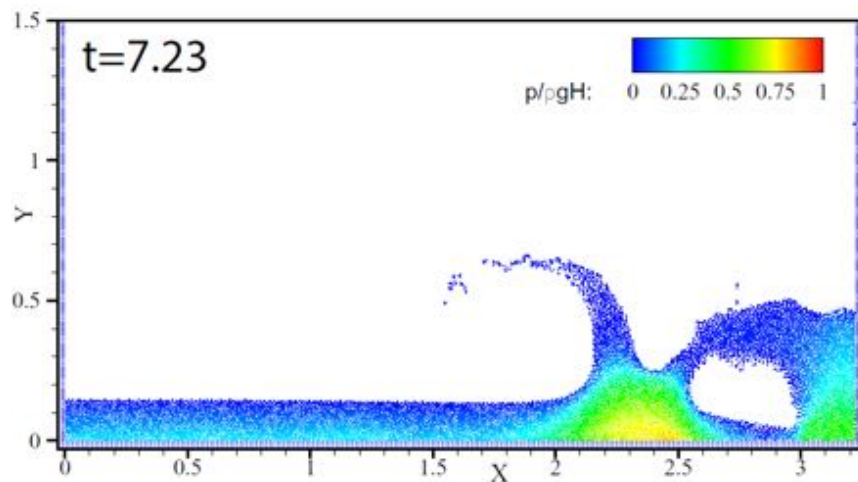
Flow visualization: streamlines



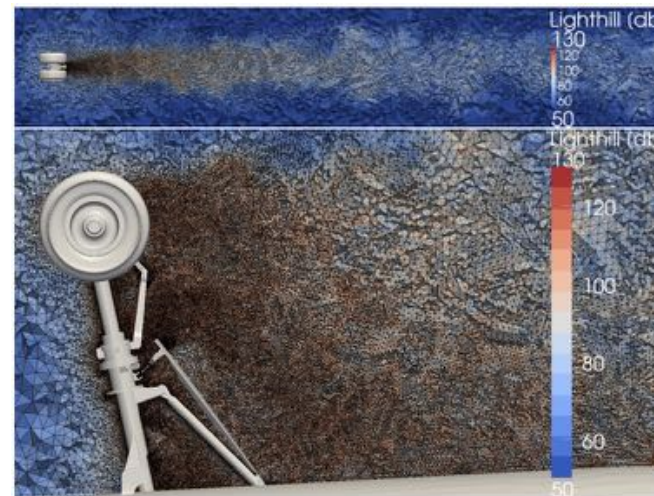
<https://www3.nd.edu/~cwang11/2dflowvis.html>

Representation of fluid flow

- Pathlines vs Streamlines
- Particles vs mesh/fixed coordinate system
- Lagrangian vs Eulerian representation
- Smooth particle hydrodynamics vs Finite element method

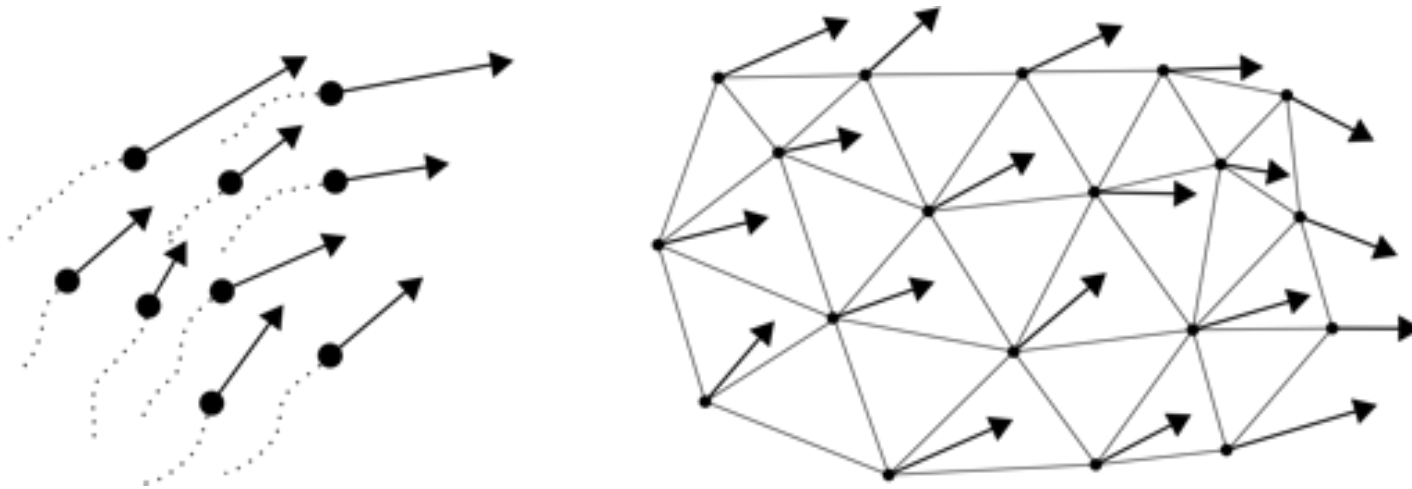


[<https://www3.nd.edu/~cwang11/2dflowvis.html>]



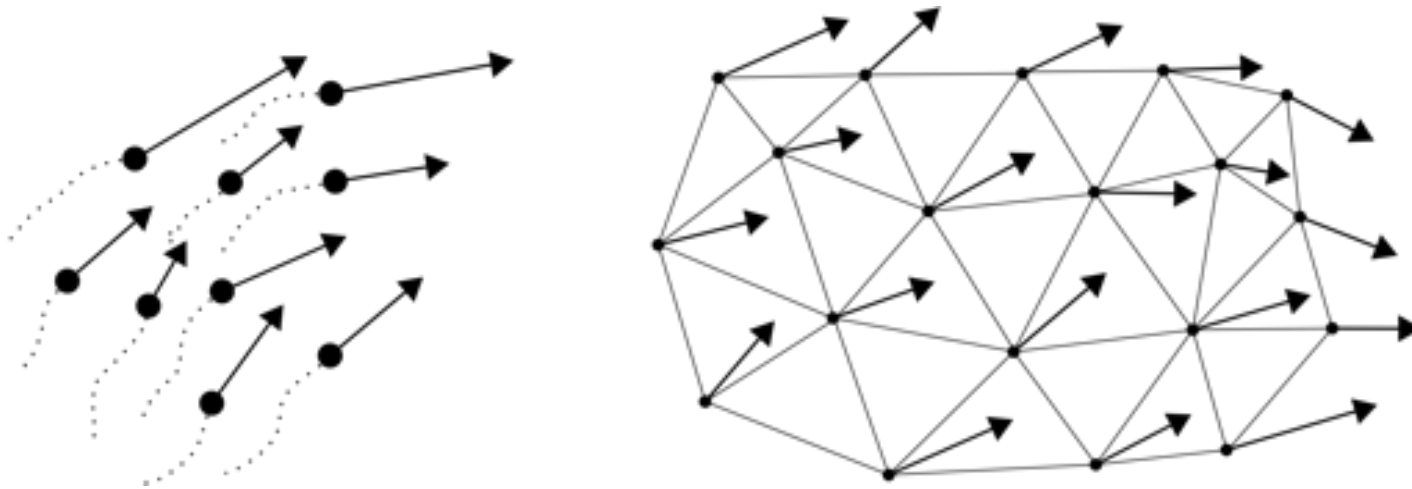
Representation of fluid flow

- Pathlines vs Streamlines
- Particles vs mesh/fixed coordinate system
- Lagrangian vs Eulerian representation
- Smooth particle hydrodynamics vs Finite element method



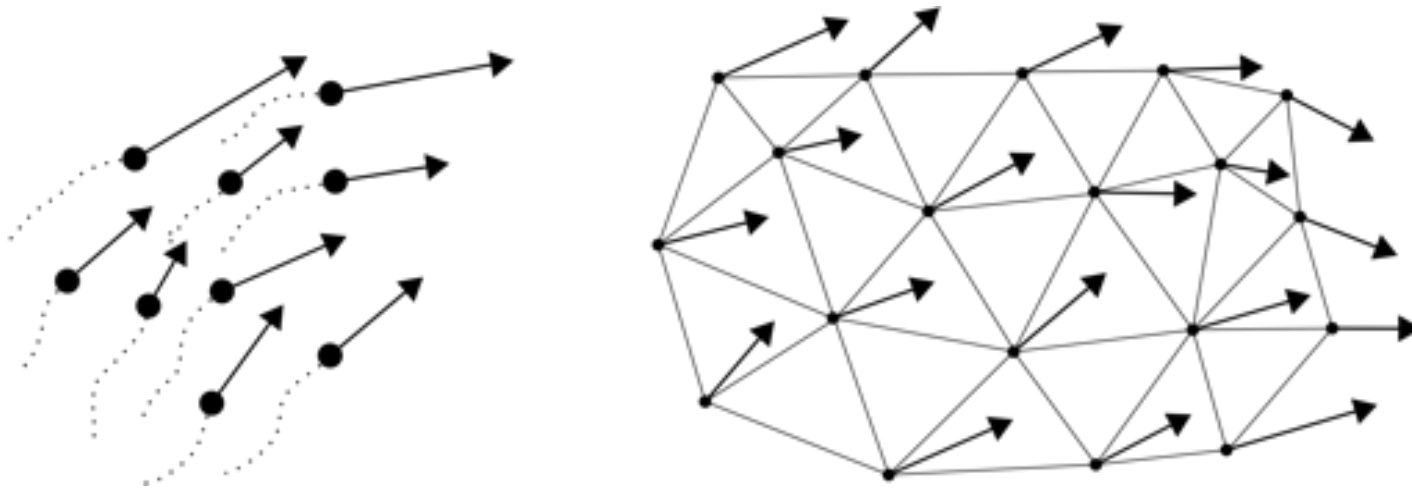
Representation of fluid flow

- Lagrangian representation: moving particle position $X(t)$, $X(0) = X_0$
- Eulerian representation: fixed position x , velocity $u(x, t)$



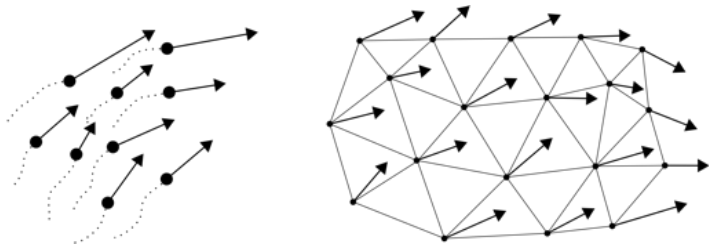
Representation of fluid flow

- Lagrangian representation: moving particle position $X(t)$, $X(0) = X_0$
- Eulerian representation: fixed position x , velocity $u(x, t)$
- $u(X(t), t) = \frac{dX}{dt}$



Representation of fluid flow

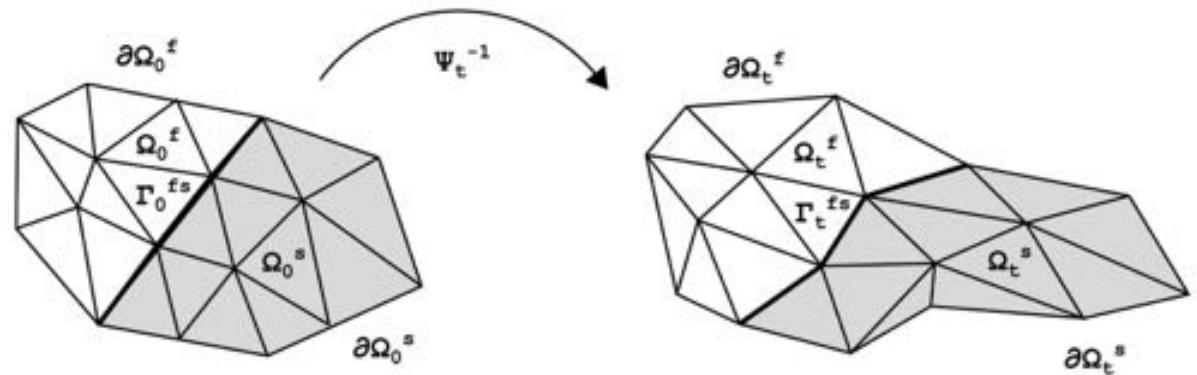
- Lagrangian representation: moving particle position $X(t)$, $X(0) = X_0$
- Eulerian representation: fixed position x , velocity $u(x, t)$
- $u(X(t), t) = \frac{dX}{dt}$
- $\frac{Du}{Dt} = \left(\frac{dX}{dt} \cdot \nabla \right) u + \frac{\partial u}{\partial t} = \frac{\partial u}{\partial t} + (u \cdot \nabla)u$
- Acceleration along particle path



Fluid-structure interaction (FSI)

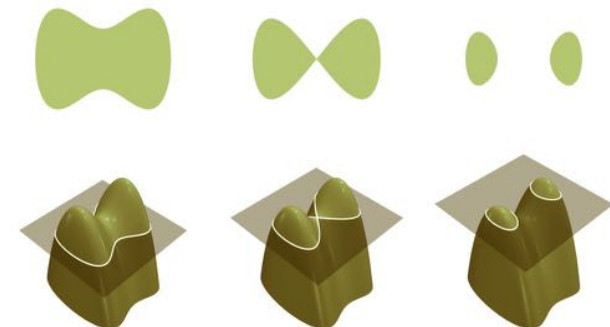
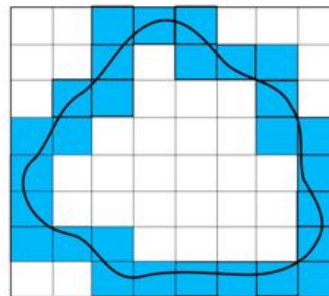
Interface tracking

- Mesh follow deformation
- Explicit interface representation



Interface capturing

- Mesh fixed
- Implicit interface representation



[https://en.wikipedia.org/wiki/Level-set_method#/media/File:Level_set_method.png]

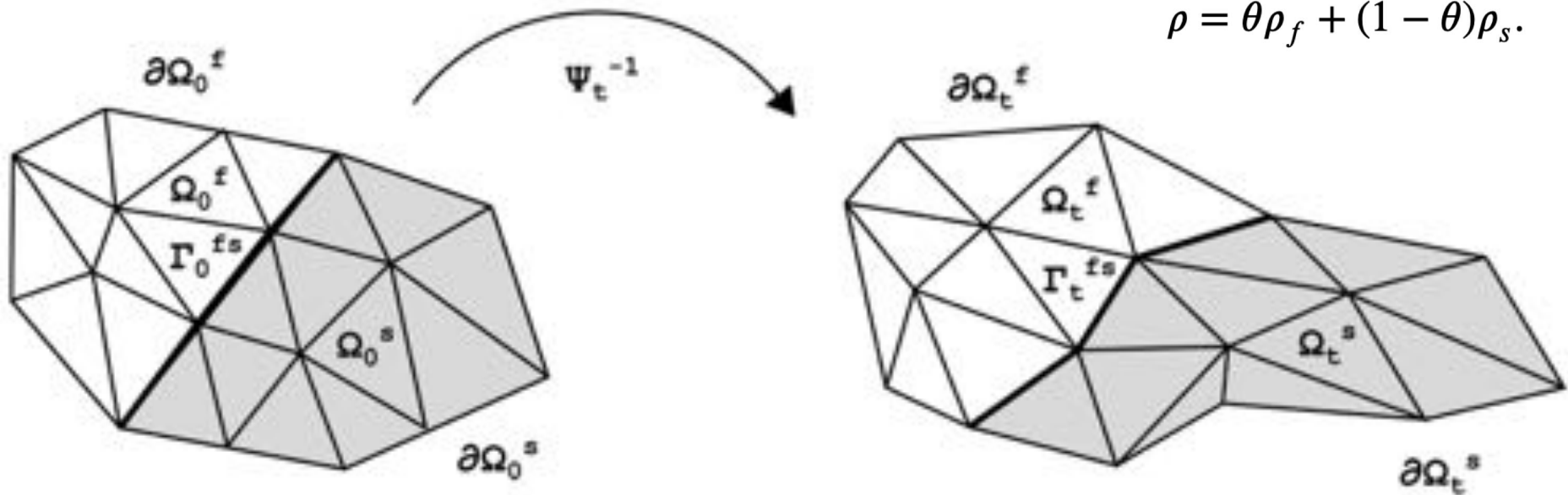
Unified continuum fluid-structure interaction

$$\begin{aligned}\rho(\dot{\mathbf{u}} + ((\mathbf{u} - \mathbf{m}) \cdot \nabla)\mathbf{u}) + \nabla p - \nabla \cdot \boldsymbol{\tau} &= \rho \mathbf{f}, & (\mathbf{x}, t) \in \Omega_t \times I \\ \nabla \cdot \mathbf{u} &= 0, & (\mathbf{x}, t) \in \Omega_t \times I\end{aligned}$$

$$\theta(\mathbf{x}, t) = \begin{cases} 1, & \mathbf{x} \in \Omega_t^f, \\ 0, & \mathbf{x} \in \Omega_t^s, \end{cases}$$

$$\boldsymbol{\tau} = \theta \boldsymbol{\tau}_f + (1 - \theta) \boldsymbol{\tau}_s,$$

$$\rho = \theta \rho_f + (1 - \theta) \rho_s.$$

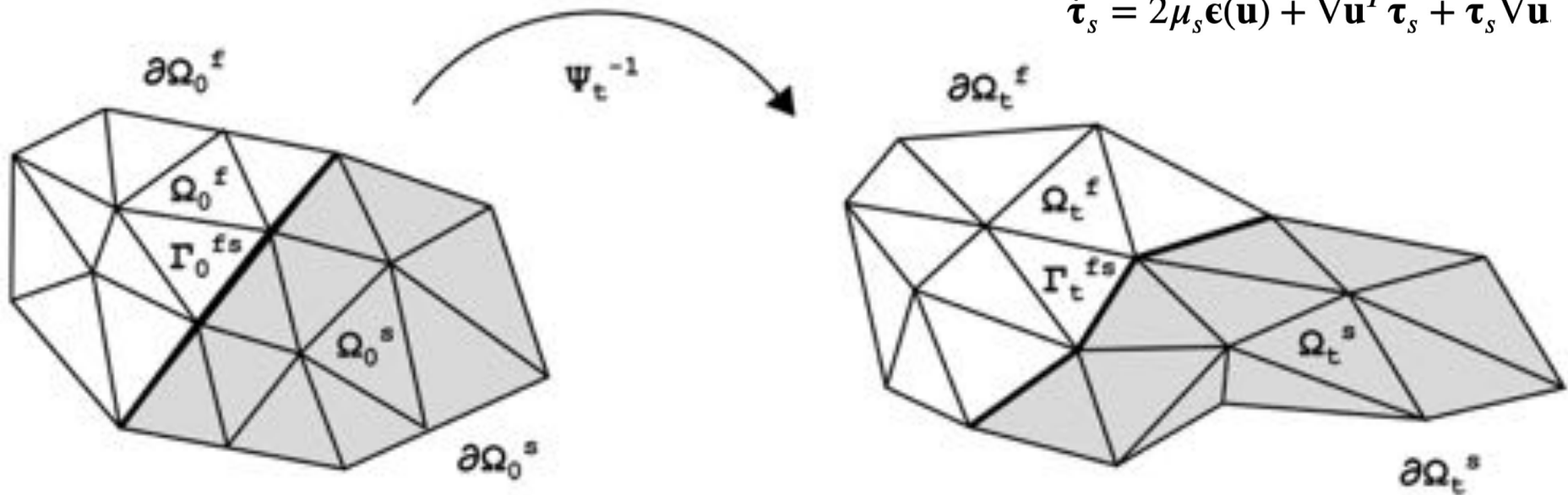


Unified continuum fluid-structure interaction

$$\begin{aligned}\rho(\dot{\mathbf{u}} + ((\mathbf{u} - \mathbf{m}) \cdot \nabla)\mathbf{u}) + \nabla p - \nabla \cdot \boldsymbol{\tau} &= \rho \mathbf{f}, & (\mathbf{x}, t) \in \Omega_t \times I \\ \nabla \cdot \mathbf{u} &= 0, & (\mathbf{x}, t) \in \Omega_t \times I\end{aligned}$$

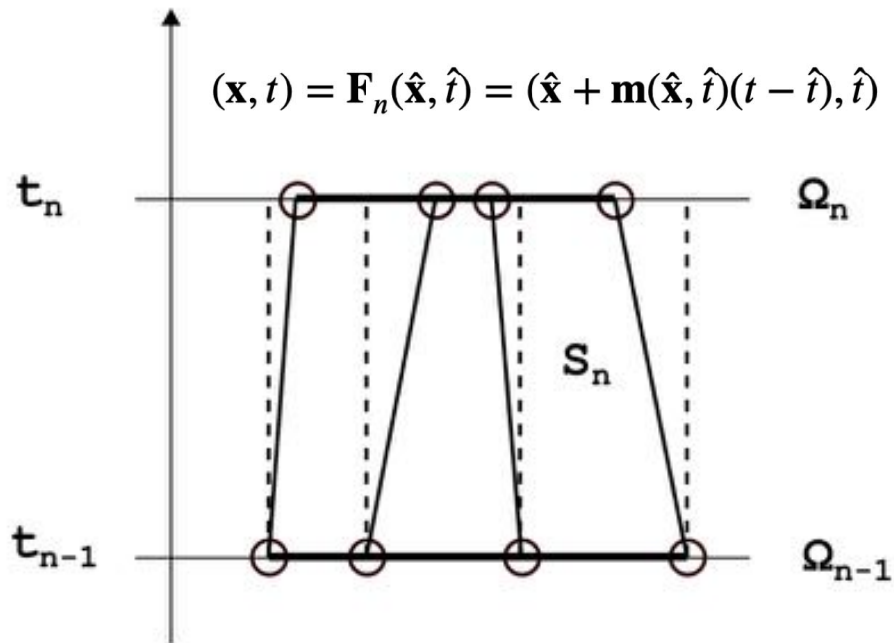
$$\boldsymbol{\tau}_f = 2\mu_f \boldsymbol{\epsilon}(\mathbf{u}), \quad \boldsymbol{\epsilon}(\mathbf{u}) = \frac{1}{2}(\nabla \mathbf{u} + \nabla \mathbf{u}^T)$$

$$\dot{\boldsymbol{\tau}}_s = 2\mu_s \boldsymbol{\epsilon}(\mathbf{u}) + \nabla \mathbf{u}^T \boldsymbol{\tau}_s + \boldsymbol{\tau}_s \nabla \mathbf{u}$$



Space-time finite element approximation

$$\hat{V}_{h,n}^{(k,m)}(\hat{S}_n) = \{\hat{v}(\mathbf{x}, t) : \hat{v} \in V_h^{(k)}(\Omega_{n-1}) \text{ for each } t \in I_n, \text{ and } \hat{v} \in P^m(I_n) \text{ for each } \mathbf{x}_{n-1} \in \Omega_{n-1}\}$$



$$V_{h,n}^{(k,m)}(S_n) = \{v(\mathbf{x}, t) = \hat{v}(\mathbf{F}_n^{-1}(\mathbf{x}, t), t) : \hat{v} \in \hat{V}_{h,n}^{(k,m)}(\hat{S}_n)\}$$

$$W_h^{(k,m)}(Q) = \{v : v|_{S_n} \in V_{h,n}^{(k,m)}(S_n)\}$$

$$V_h^{(k,m)}(Q) = \{v \in W_h^{(k,m)}(Q) : v \in C(\bar{Q})\}$$

Space-time finite element approximation

find $\mathbf{U} \in [V_{h,g_D}^{(1,1)}(Q)]^d$ and $P \in W_h^{(1,0)}(Q)$, such that

$$\begin{aligned} (\rho(\dot{\mathbf{U}} + ((\mathbf{U} - \mathbf{M}) \cdot \nabla)\mathbf{U}), \mathbf{v})_Q + (\mu_f \boldsymbol{\epsilon}(\mathbf{U}), \boldsymbol{\epsilon}(\mathbf{v}))_{Q_f} + (\mathbf{T}, \nabla \mathbf{v})_{Q_s} - (P, \nabla \cdot \mathbf{v})_Q + (q, \nabla \cdot \mathbf{U})_Q \\ + (\mathbf{g}_N, \mathbf{v})_{\partial Q_N} + SD_\delta(\mathbf{U}, \mathbf{M}, P; \mathbf{v}, q) = (\rho \mathbf{f}, \mathbf{v})_Q, \end{aligned}$$

for all $\mathbf{v} \in [W_{h,0}^{(1,0)}(Q)]^d$ and $q \in W_h^{(1,0)}(Q)$.

$$W_h^{(k,m)}(Q) = \{v : v|_{S_n} \in V_{h,n}^{(k,m)}(S_n)\}.$$

$$V_h^{(k,m)}(Q) = \{v \in W_h^{(k,m)}(Q) : v \in C(\bar{Q})\}$$

Mesh smoothing – elastic analogy

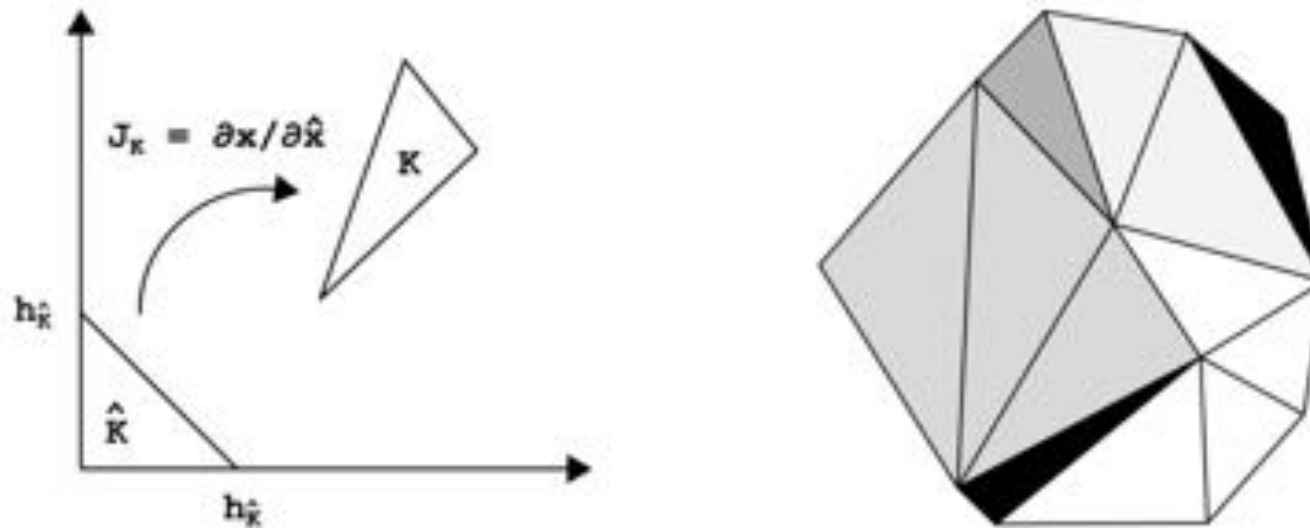
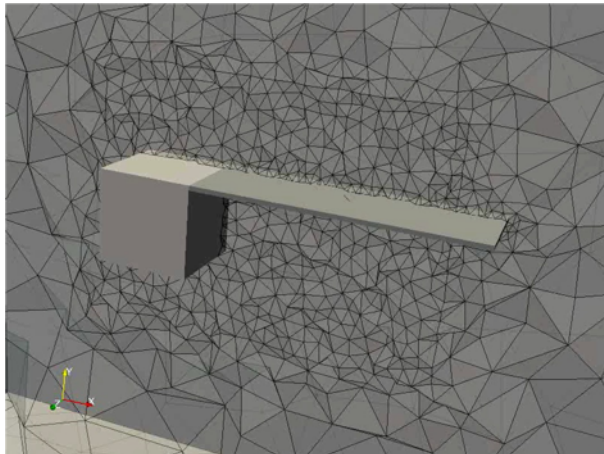


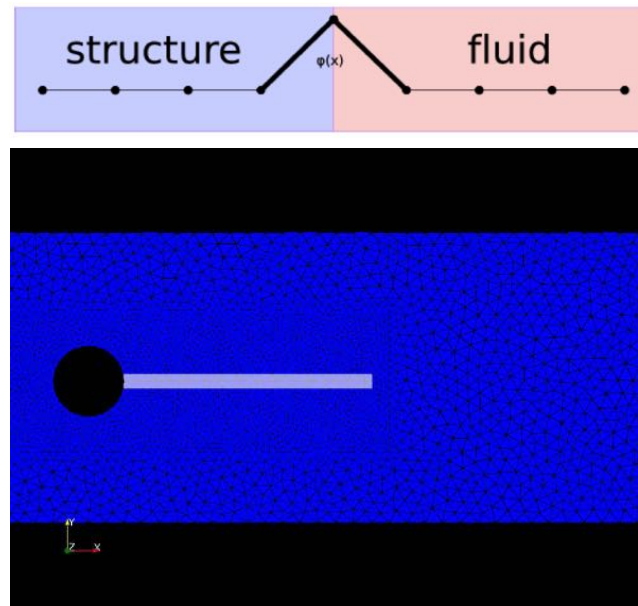
FIGURE 3 Map from a reference triangle \hat{K} to an element K and its associated Jacobian J_K (left), and a triangle mesh with each element K coloured based on its quality measure $Q(K)$, with darker colours for higher values (right).

Unified Continuum fluid-structure interaction



ALE-FEM method

- Conforming fluid-solid mesh
- Mesh smoothing



[J. Hoffman, J. Jansson, M. Stöckli, M3AS, Vol.21(3), 2011.]

Contact model

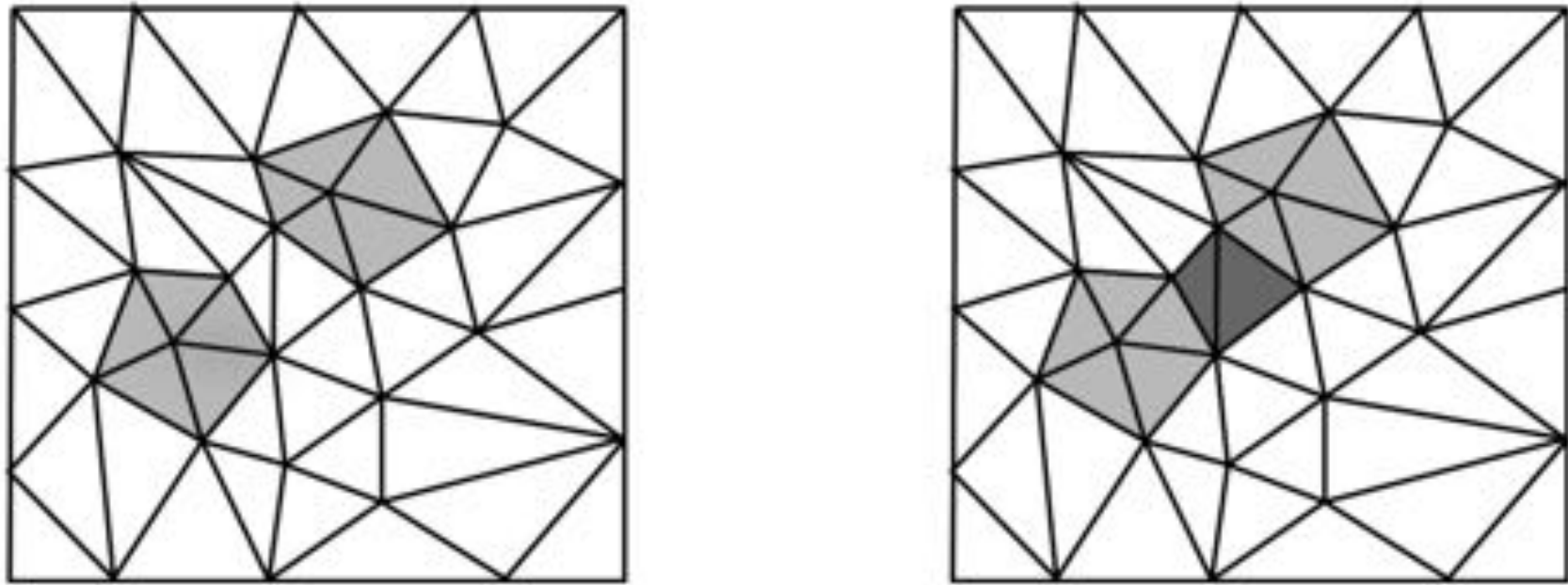
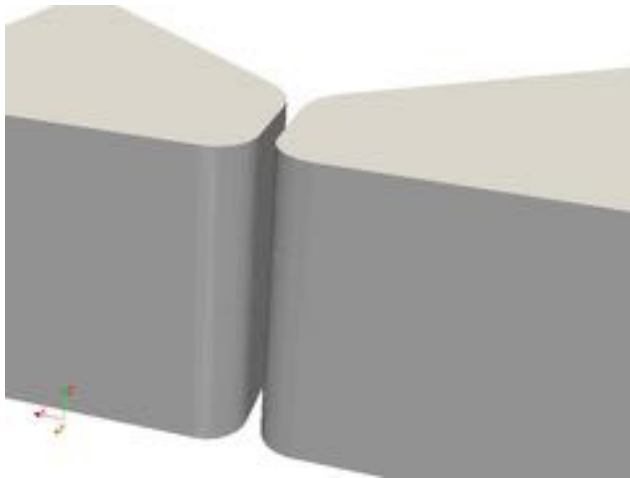


FIGURE 4 Illustration of the UC-FSI contact model, where collision is detected between two structure domains marked by a light shade of grey (left), which then activates a phase change in the contact region marked in a darker shade of grey (right).

Unified Continuum contact model

[Spühler, Degirmenci, Jansson, Hoffman, KTH PhD thesis, 2018]

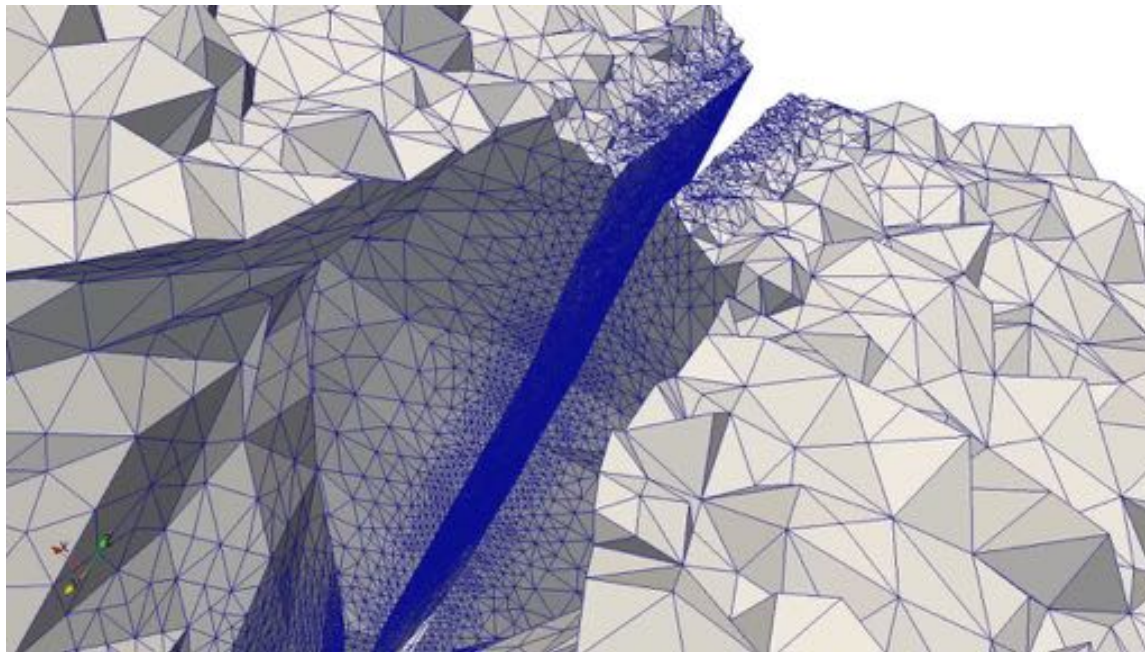


Algorithm 1 *Contact algorithm*

1. Mark all cells K as non-contact.
2. Solve the Eikonal equation $|\nabla D| = 1$ using a artificial viscosity stabilized cG(1) method with $D = 0$ on the boundary Γ and in the structure subdomain Ω_s for the distance $D = D(x)$.
3. Compute $|\nabla D|$, and define the medial axis M as: $M = \{x \mid |\nabla D(x)| \leq \gamma\}$, with the threshold parameter $\gamma < 1$.
4. Define the contact medial axis: $\hat{M} = \{x \mid x \in M, x \notin \Omega_s, D(x) < \alpha \hat{h}\}$, with \hat{h} the minimum cell size in the mesh.
5. Solve the Eikonal equation $|\nabla D_{\hat{M}}| = 1$ using an artificial viscosity stabilized cG(1) method with $D_{\hat{M}} = 0$ on the contact medial axis \hat{M} for the distance from \hat{M} $D_{\hat{M}} = D_{\hat{M}}(x)$.
6. Mark all fluid cells as contact which fulfill: $C = \{x \mid D_{\hat{M}} \leq \beta \hat{h}\}$

FSI simulation of vocal folds

[N.C.Degirmenci, et al, Proc. Interspeech, 2017]



Navier-Stokes Brinkman model

$$\rho \left(\frac{\partial}{\partial t} \mathbf{u} + \mathbf{u} \cdot \nabla \mathbf{u} \right) - \nabla \cdot \boldsymbol{\sigma}(\mathbf{u}, p) + \frac{\mu}{K}(\mathbf{u} - \mathbf{u}_s) = 0 \quad \text{in } \mathbb{R}^+ \times \Omega \quad (1)$$

$$\nabla \cdot \mathbf{u} = 0 \quad \text{in } \mathbb{R}^+ \times \Omega \quad (2)$$

$$\mathbf{u} = 0 \quad \text{on } \Gamma_{\text{noslip}} \quad (3)$$

$$\boldsymbol{\sigma} \mathbf{n} - \rho \beta (\mathbf{u} \cdot \mathbf{n}) \mathbf{n} = \mathbf{h} \quad \text{on } \Gamma_{\text{outflow}} \quad (4)$$

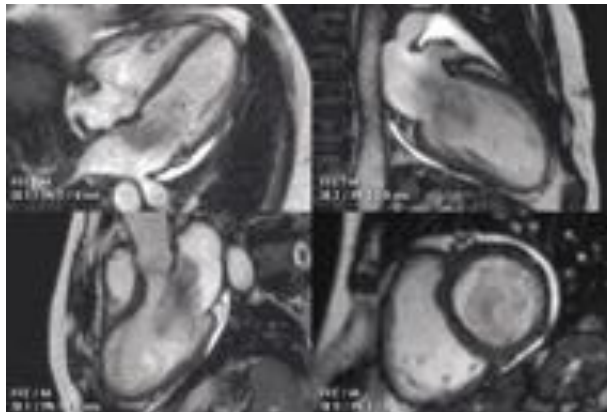
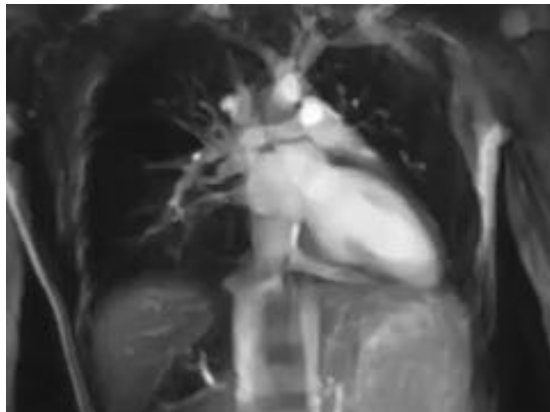
$$\mathbf{u} = \mathbf{g} \quad \text{on } \Gamma_{\text{inflow}} \quad (5)$$

$$\mathbf{u}|_{t=0} = \mathbf{u}_0 \quad (6)$$

Here $p(\mathbf{x}, t)$ and $\mathbf{u}(\mathbf{x}, t)$ represent the fluid pressure and the flow velocity respectively, μ is the dynamic viscosity and ρ the density. The volume penalization term $\frac{\mu}{K(t, \mathbf{x})} \mathbf{u}(t, \mathbf{x})$ is commonly known as *Darcy drag* which is characterized by the permeability $K(t, \mathbf{x})$.

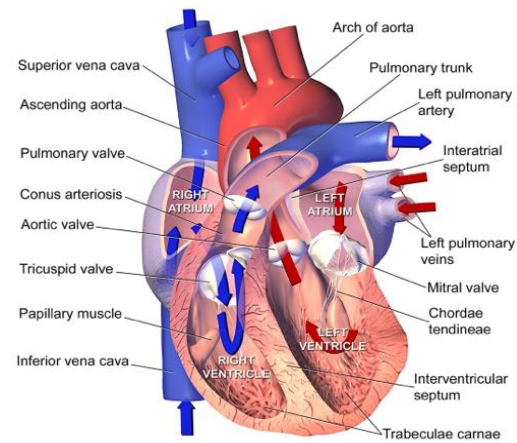
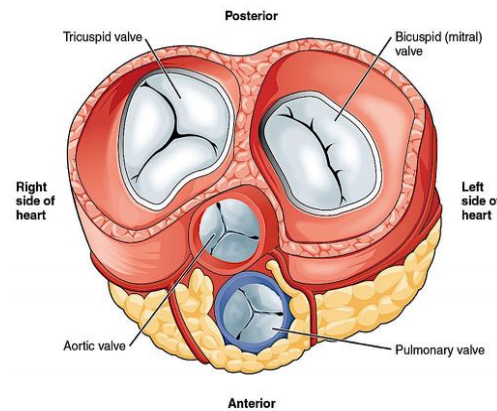
The left ventricle of the heart

- The LV pumps the blood through the aorta and experiences the highest forces, and the most problems.
- In vivo imaging include ultrasound, MRI, CT.
- Tissue is easier to image than the blood flow, blood pressure.
- Two phases: **systole** (contract) and **diastole** (relax)



The left ventricle of the heart

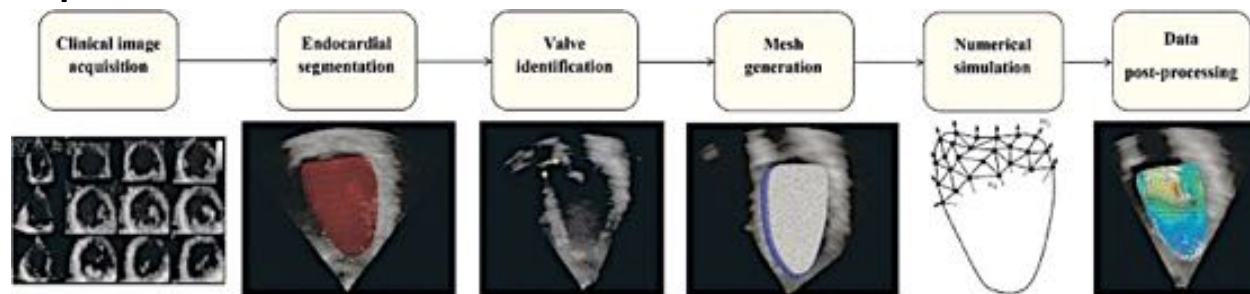
- **Regurgitation** is the name for leaking heart valves.
- **Stenosis** is the term for a valve that doesn't open properly.
- **Thrombosis** is the formation of a blood clot, which may block the blood supply to cause a heart attack or stroke.



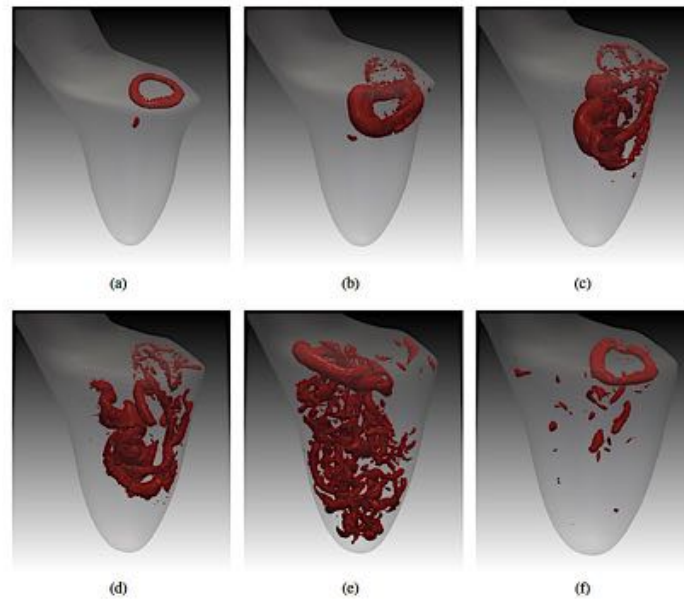
Sectional Anatomy of the Heart

Patient-specific LV blood flow simulation

- 4DTTE images, semi-automated segmentation
- Valves identified by sonographer
- Mesh generation by ANSA (BETA CAE Systems)
- >200 patients processed to date.

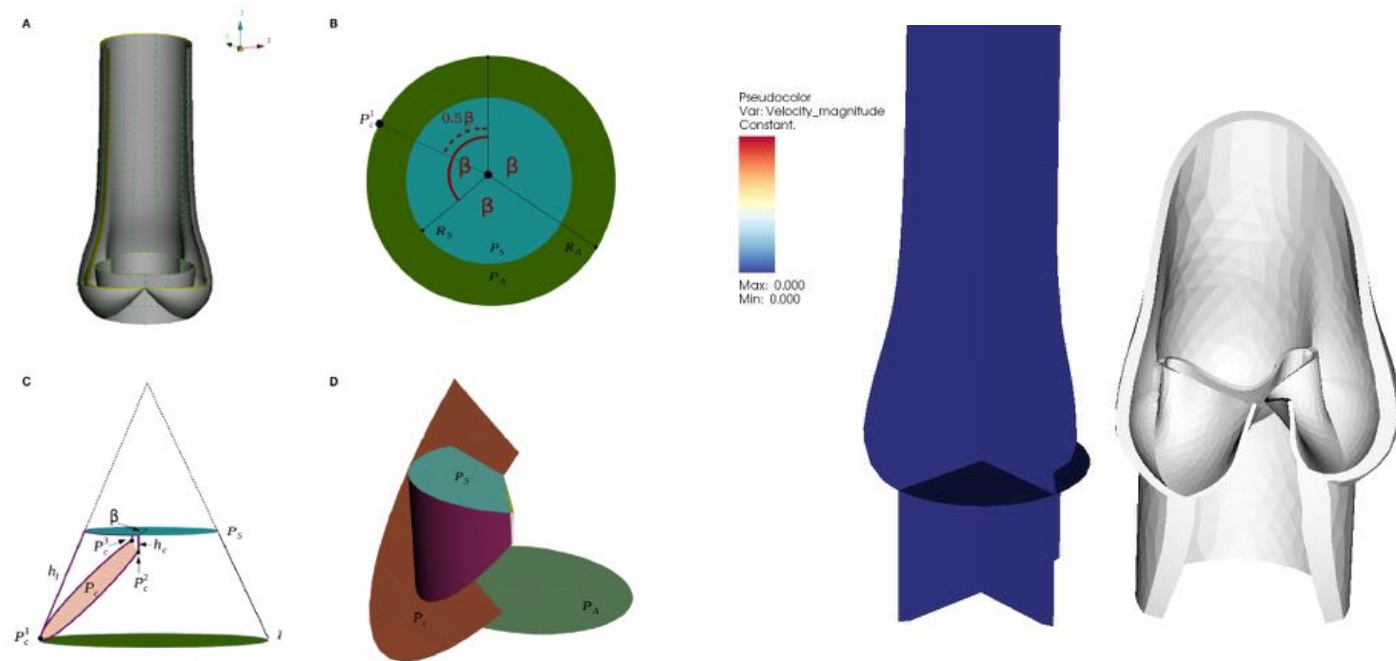


Patient-specific LV blood flow simulation

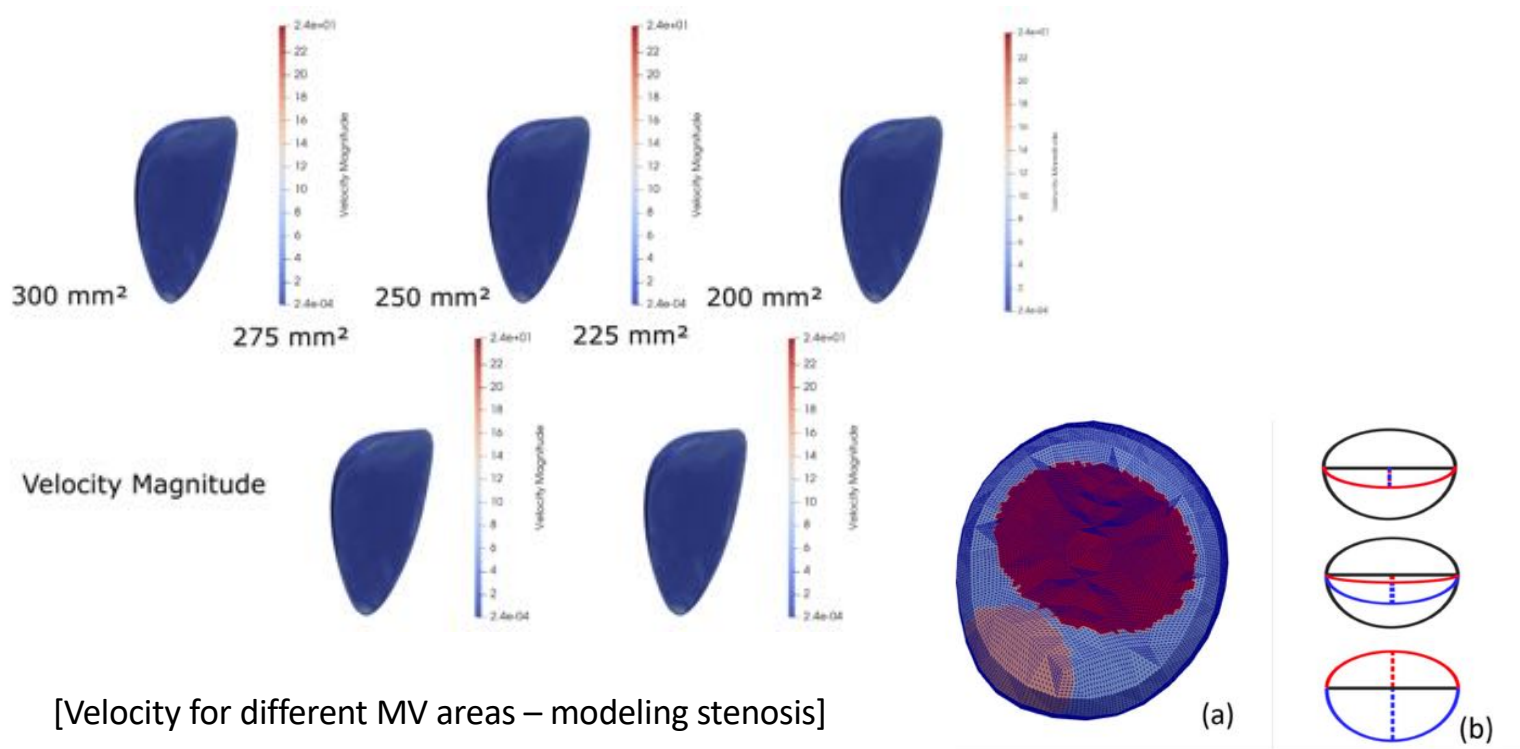


[Visualization by evolving lambda2 isosurfaces]

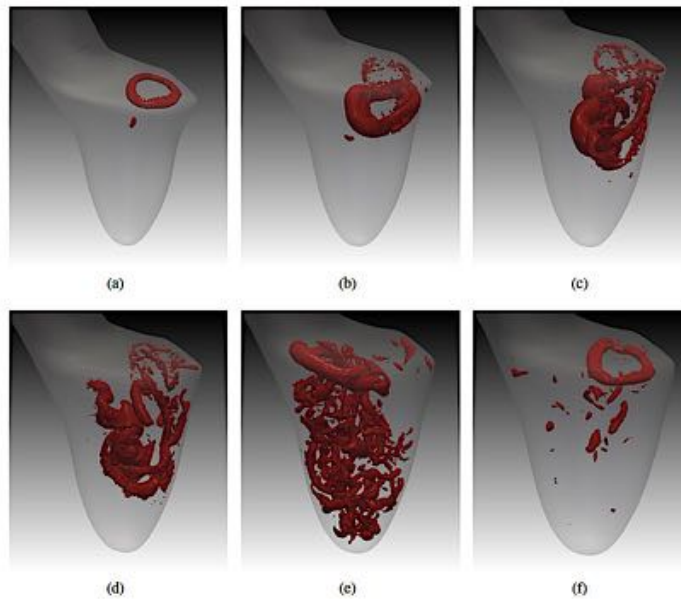
Systole: FSI simulation of 3D aortic valves



Diastole: 2D mitral valve model



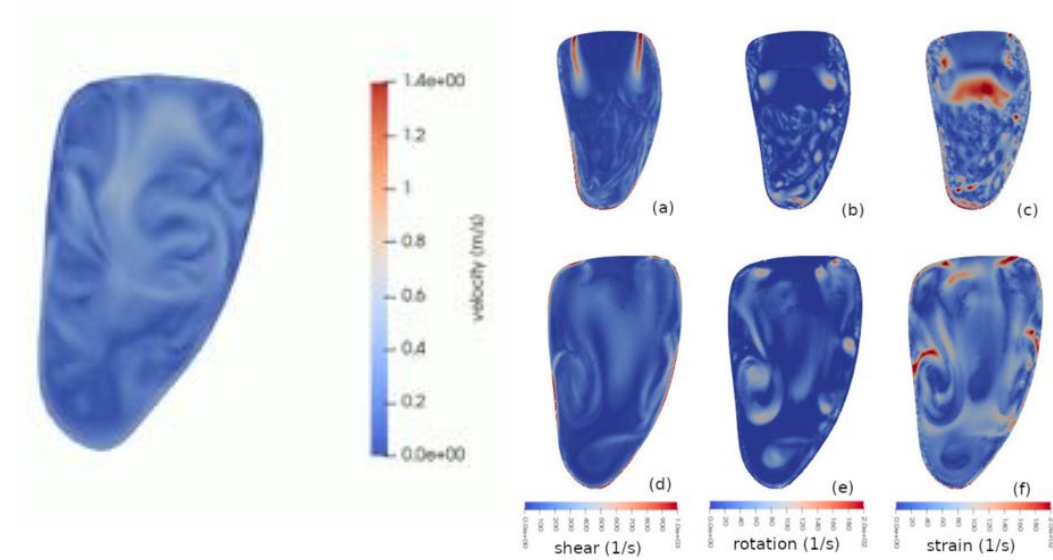
Analysis of LV turbulent flow structures



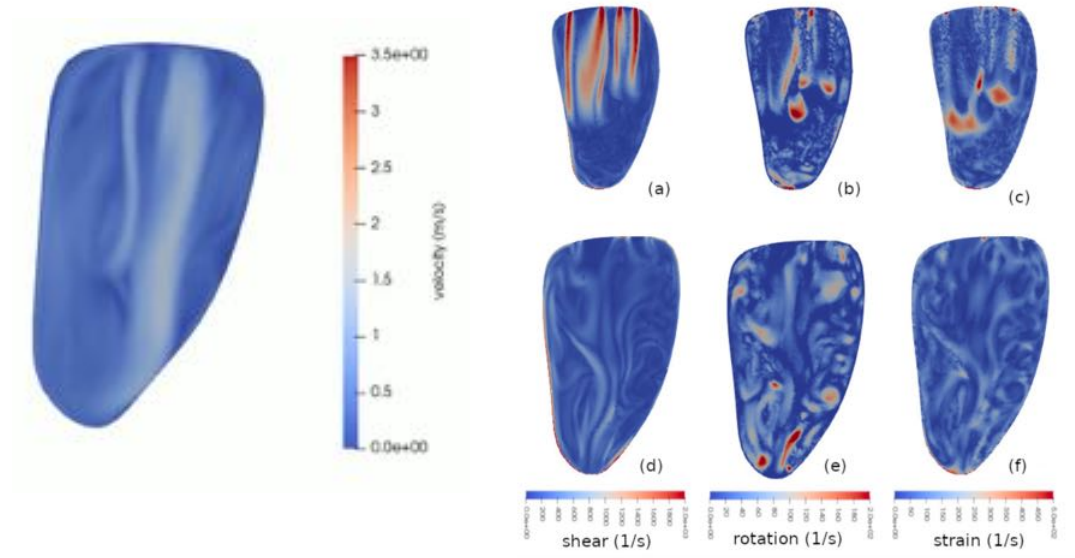
[Visualization by evolving lambda2 isosurfaces]



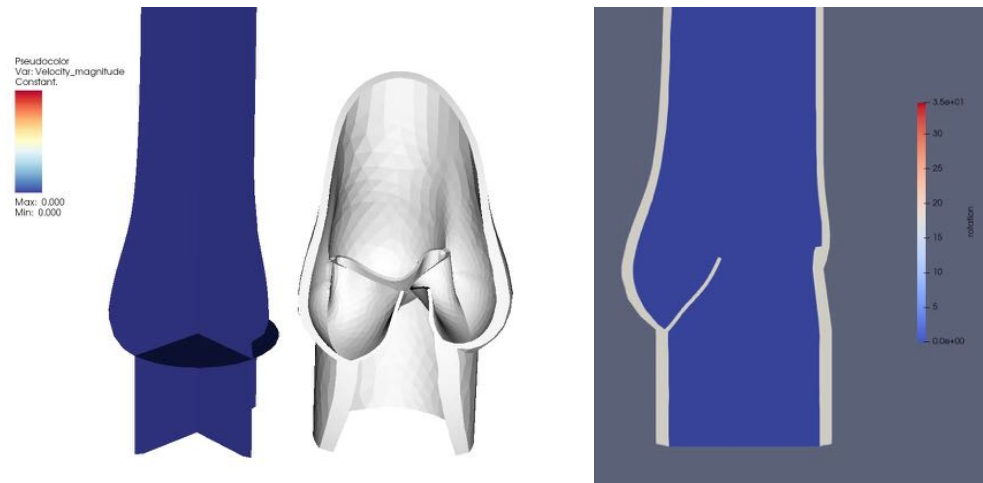
LV simulation (local Frobenius norms)



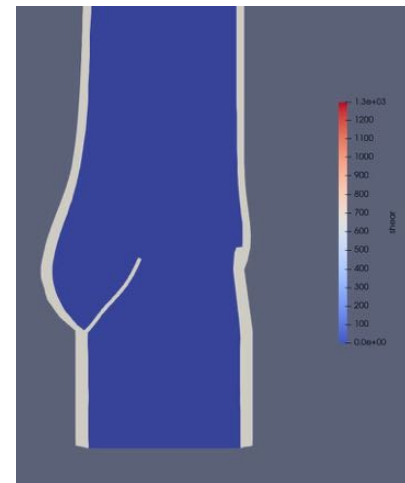
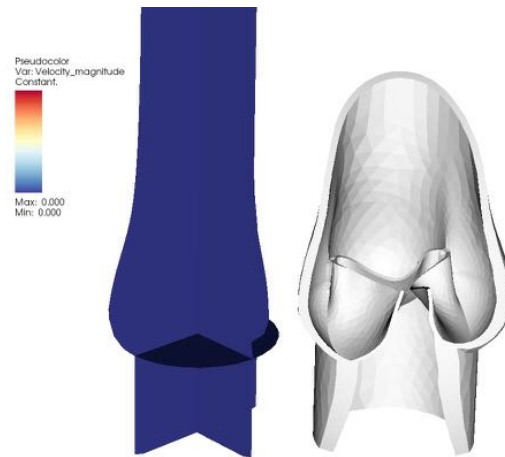
LV simulation (local Frobenius norms)



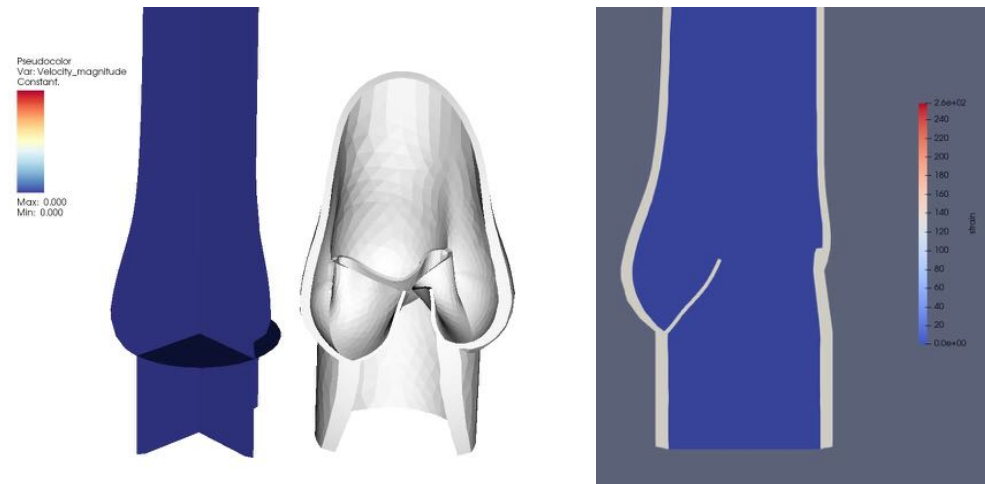
Aortic valve - rotation



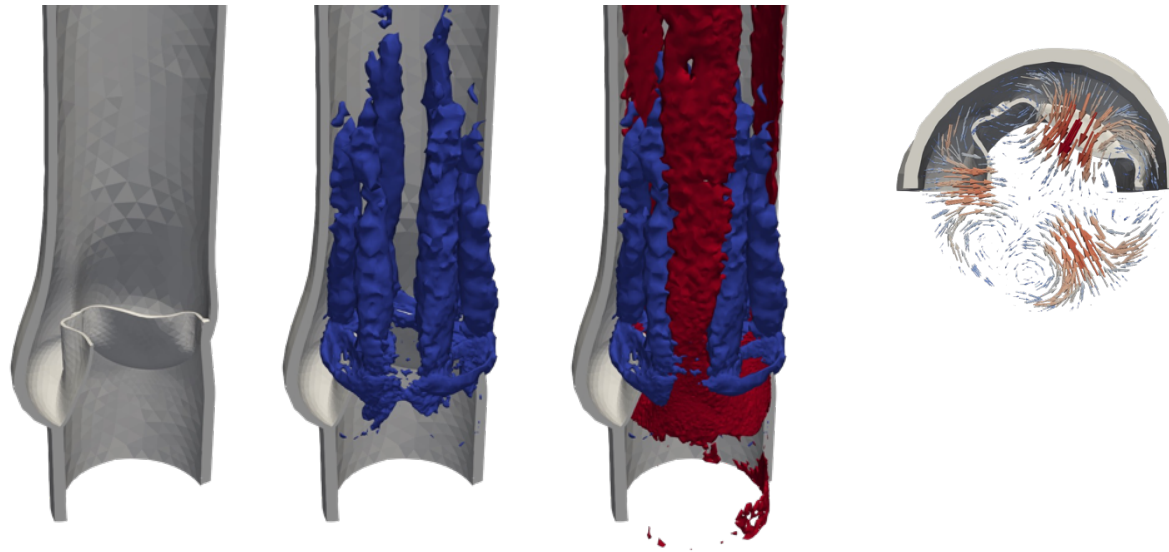
Aortic valve - shear



Aortic valve- strain



Aortic valve: rotation, rotation + shear



Models for shear-induced platelet activation

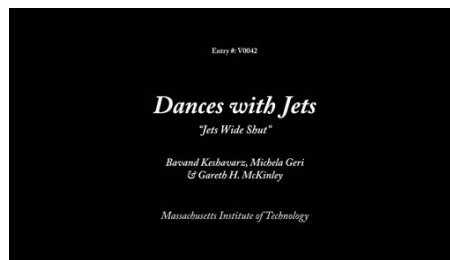
- The triple decomposition of the velocity gradient tensor separates the flow into the components of pure strain, rigid body rotation and shear.
- CFD models for shear-induced platelet activation are typically based on the strain rate tensor.
- The strain rate tensor does not distinguish between strain and shear flow.
- The triple decomposition offers a method to separate shear from strain, which can lead to more precise models for shear-induced platelet activation.

Nasa CFD Vision 2030

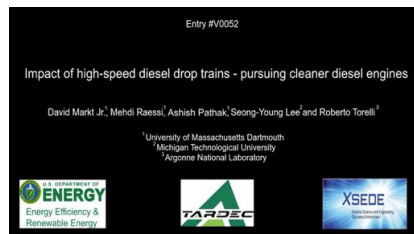
CFD TECHNOLOGY GAPS AND IMPEDIMENTS

- Effective Utilization of High-Performance Computing (HPC)
- Unsteady Turbulent Flow Simulations Including Transition to Turbulence and Separation
- Autonomous and Reliable CFD Simulation
- Knowledge Extraction and Visualization
- Multidisciplinary/Multiphysics Simulations and Frameworks

Multiphase flow



- <https://gfm.aps.org/meetings/dfd-2020/5f5ec1d2199e4c091e67bd66>



- <https://gfm.aps.org/meetings/dfd-2020/5f5f6542199e4c091e67be2a>

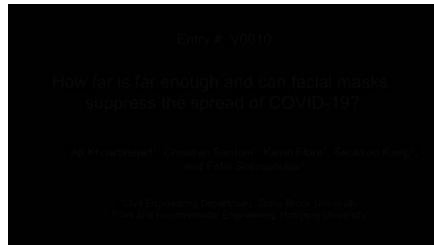
Multiphase flow



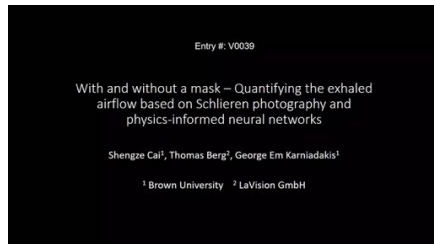
- <https://gfm.aps.org/meetings/dfd-2020/5f5fc002199e4c091e67bf49>

Gallery of fluid motion

Ex. COVID spread with and without mask: differential equations vs deep learning



<https://gfm.aps.org/meetings/dfd-2020/5f4fe574199e4c091e67ba6e>



<https://gfm.aps.org/meetings/dfd-2020/5f5e6ef8199e4c091e67bd37>

Credits

Gallery of fluid motion (American Physical Society)

- <https://gfm.aps.org>

Album of fluid flow (Milton Van Dyke)

- https://en.wikipedia.org/wiki/An_Album_of_Fluid_Motion
- <https://www.abebooks.com/9780915760022/Album-Fluid-Motion-Milton-Dyke-0915760029/plp>

References



- Hoffman, Energy stability analysis of turbulent incompressible flow based on the triple decomposition of the velocity gradient tensor, Physics of Fluids, Vol.33(8), 2021.



- Kronborg et al., Computational analysis of flow structures in turbulent ventricular blood flow associated with mitral valve intervention, Frontiers in Physiology, Frontiers in Physiology, 2022.



- Kronborg and Hoffman, The triple decomposition of the the velocity gradient tensor as a standardized Schur form, Physics of Fluids, Vol.35(3), 2023.

New SIAM book

